International Journal of

Informatics Society

Informatics Society

Aims and Scope

The purpose of this journal is to provide an open forum to publish high quality research papers in the areas of informatics and related fields to promote the exchange of research ideas, experiences and results.

Informatics is the systematic study of Information and the application of research methods to study Information systems and services. It deals primarily with human aspects of information, such as its quality and value as a resource. Informatics also referred to as Information science, studies the structure, algorithms, behavior, and interactions of natural and artificial systems that store, process, access and communicate information. It also develops its own conceptual and theoretical foundations and utilizes foundations developed in other fields. The advent of computers, its ubiquity and ease to use has led to the study of informatics that has computational, cognitive and social aspects, including study of the social impact of information technologies.

The characteristic of informatics' context is amalgamation of technologies. For creating an informatics product, it is necessary to integrate many technologies, such as mathematics, linguistics, engineering and other emerging new fields.

Guest Editor's Message

Yu Enokibori

Guest Editor of Thirtieth Issue of International Journal of Informatics Society

We are delighted to have the thirtieth issue of the International Journal of Informatics Society (IJIS) published. This issue includes selected papers from the Ninth International Workshop on Informatics (IWIN2017), which was held at Zagreb, Croatia, Sept. 3-6, 2017. The workshop was the eleventh event for the Informatics Society, and was intended to bring together researchers and practitioners to share and exchange their experiences, discuss challenges and present original ideas in all aspects of informatics and computer networks. In the workshop 33 papers were presented in eight technical sessions. The workshop was successfully finished with precious experiences provided to the participants. It highlighted the latest research results in the area of informatics and its applications that include networking, mobile ubiquitous systems, data analytics, business systems, education systems, design methodology, intelligent systems, groupware and social systems.

Each paper submitted to IWIN2017 was reviewed in terms of technical content, scientific rigor, novelty, originality and quality of presentation by at least two reviewers. Through those reviews, 16 papers were selected for publication candidates of IJIS Journal, and they were further reviewed as Journal papers. This volume includes five papers accepted from the selected papers, which have been improved through the workshop discussion and the reviewers' comments. We have two categories in IJIS papers, Regular papers and Industrial papers, each of which were reviewed from the different points of view. The five accepted papers are categorized as 2 Regular papers and 3 Industrial papers.

We publish the journal in print as well as in an electronic form over the Internet. We hope that the issue would be of interest to many researchers as well as engineers and practitioners over the world.

Yu Enokibori received his B.E., M.E., and Ph.D. degrees in Engineering Science from Ritsumeikan University in 2005, 2007, and 2010, respectively. He became an assistant professor at Graduate School of Information Science, Nagoya University in 2015. He is now with Graduate School of Informatics, Nagoya University since 2017. His research interests include ubiquitous computing, wearable computing, invisible computing, healthcare and medical computing, and human computer interaction. He is a member of IPSJ, JSAI, SOBIM, JANS, and ACM.

Regular Paper

Discovering Hotspots Using Photographic Orientation and Angle of View from Social Media Site

Masaharu Hirota[†], Masaki Endo[‡], Daiju Kato[♯], and Hiroshi Ishikawa[*]

[†]Faculty of Informatics, Okayama University of Science, Japan
[‡]Division of Core Manufacturing, Polytechnic University, Japan
[♯] WingArc1st Inc., Japan
[*] Faculty of System Design, Tokyo Metropolitan University, Japan
[†]hirota@mis.ous.ac.jp, [‡]endou@uitec.ac.jp, [♯]kato.d@wingarc.com, [*]ishikawa-hiroshi@tmu.ac.jp

Abstract - Hotspot is interesting places for many people to do sightseeing. Visualization of hotspots reveals user interests, which is important for industries such as tourism and marketing research. Hotspot is classifiable to two types: area of interests and shooting spot. This paper introduces a new method using clustering algorithm for extracting the area of interests based on various metadata annotated with a photograph from photo-sharing sites. Although several social-based techniques for extracting hotspots have been proposed using photographic location, those most methods cluster photographs based solely on the density of geographic proximity. However, in almost cases, a hotspot and shooting point where photographs were taken are distant. Also, when a photograph was taken, an angle of view, which the breadth of a subject as seen by a camera system, was measured by a camera. Therefore, we propose to extract the area of interests using photographic location, orientation and angle of view in geo-referenced and oriented photographs. We demonstrate our approach by extracting the area of interests using photographs annotated with those metadata from Flickr.

Keywords: Area of interest, Shooting spot, Photograph location, Photograph orientation, Clustering

1 INTRODUCTION

According to the increasing popularity of mobile devices such as digital cameras and smartphones, numerous photographs taken by photographers have been uploaded to photo-sharing web services such as Flickr [21] and Panoramio [22]. Recently those devices have included embedded global positioning system (GPS). Using them, photographers can readily take photographs with photographic metadata. A photographic location which is one of a type of the metadata observed by GPS shows a place at which photographer took a photograph. Also, photographic orientation indicates the direction in which the photograph was taken from the photographic location. Particularly, photographs with a photograph-orientation feature have become numerous recently. Also, many photographs on photo-sharing sites have metadata that are annotated by users through social tagging.

Many people might take photographs of subjects or landscapes satisfying their own interests. Then, they upload those photographs to the sites. As places at which many photographs

have been taken, these locations might also be interesting places for many people to visit. In this paper, we define such places as a hotspot. Also, we can extract the interesting places using photographs obtained from photo-sharing sites. Even if it is in a famous tourism spot, all areas in the spot are not necessarily worth for sightseeing. Therefore, some methods have been proposed to extract hotspots based on photographic locations from photographs at photo-sharing sites [8], [14], [17], [23], [24]. The extracted hotspots might reflect people's interests, or be useful for marketing research, spatial analysis, and so on [13], [30]. Analyzing such areas is necessary for industries such as those related to tourism [12],[13] . Furthermore, tourist attraction recommendation systems such as [10], [12] can use this approach. By presenting hotspots to people who visit a city for the first time, our approach assists tourism.

A hotspot is classifiable into two types: area of interest (a place captured in the photographs), or shooting spot (a place to take photographs). Figure 1 shows examples of shooting spots and area of interests. In Fig. 1, the gray circle shows photographic location. The break line shows pseudo triangle calculated by the photographic orientation and angle of view. The cell surrounded by a solid line represents a part of the area. Also, the cell filled by gray shows shooting spots, and an area of interest. We define a shooting spot as one type of hotspot in . When a photographer takes a photograph of attractive spots such as landmarks or landscapes, they take the photographs at a place which is distant from the spots. Also, an area of interest (or point of interest) of the other type of a hotspot is attractive as tourist spots for many people (e.g., Colosseum, Statue of Liberty). In such areas, many photographers take a lot of photographs inside or nearby from distant places. Such places are also extracted as hotspots and are defined as an area of interest. In addition, hotspots occur because of an event that might occur. When an event such as reworks display happens, many people take photographs related to the event.

Although many methods to extract and visualize the area of interest from photo-sharing sites have been proposed, those studies extract area of interest using photographic location where photographs were taken. Almost researchers to discover area of interests extract places where the density of photographic location is higher than other places using the density-based clustering algorithm like Density-based spatial
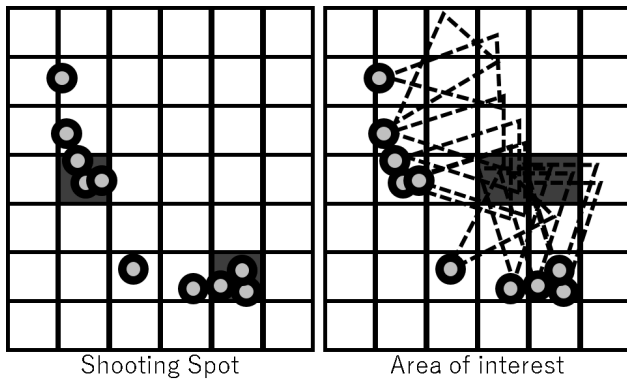
Figure 1: Example of area of interest and shooting spot using photographic location and pseudo triangle.

clustering of applications with noise (DBSCAN) [5] and P-DBSCAN [5].

However, in almost case, a photographic subject of a photograph is several meters away from a place where a photographer took the photo, like Fig. 1. As a result, a place extracted based on the density of photographic location is not the area of interest, but shooting spot. Therefore, we extract area of interests using photographic orientation and angle of view of a photograph. Modern cameras and smartphones equipped with a digital compass can add the metadata of photographic orientation taken by a user. Photographic orientation presents the direction in which the photograph was taken. Also, the angle of view is the angular degree of a given scene that is included in the photograph taken with a camera.

In this paper, we propose a novel clustering method to extract area of interests using photographic orientation and angle of view. In our approach, we use pseudo triangle which is created by the photographic orientation and angle of view. We classify the area into an area of interest or not based on the degree of overlap of the triangles.

The remainder of the paper is organized as follows. Section 2 presents works related to extracting hotspots and area of interests. Section 3 presents a description of our proposed method to extract area of interests using photographic orientation and angle of view. Section 4 explains several examples of our proposed system and presents a discussion of the results. Section 5 concludes the paper with a discussion of results and future works.

2 RELATED WORKS

2.1 Clustering Algorithms to Extract Hotspots

Some methods have been proposed to extract hotspots from the many photographs with the photographic location which are available on photo sharing sites. There are two main approaches to extract hotspots using the photographic location.

First approach is the density-based clustering algorithm such as DBSCAN [5] or mean shift [40] to extract hotspots from a dataset which includes huge photographs annotated with photographic location. Crandall et al. presented a method to extract hotspots using mean shift based on many photographs annotated with photographic location from the photo-sharing site [4]. Kisilevich et al. proposed P-DBSCAN, which a density-based clustering method improved DBSCAN for the

definition of reachable point, to extract hotspots using the density of photographic locations [8]. Ankerst et al. proposed a clustering method of OPTICS which is a variation of DB-SCAN to create a cluster using different subspaces extracted from various parameter [34]. Sander et al. proposed GDB-SCAN of generalized DBSCAN which extends to enable the corresponding to both spatial and their non-spatial features [33]. Shi et al. proposed density-based clustering method to extract places of interest using spatial information and the social relationships between users [24].

The other approach to extract hotspots is grid-based clustering algorithm. Grid-based clustering is that the data space is quantized into a finite number of cells which is formed by the grid structure. Also, in the grid-based clustering, identifying which a cell is a cluster or not is the number of data included in the cell. The main advantage of the algorithm of grid-based clustering is a fast processing time, which most of the algorithms achieve a time complexity $O(n)$ of where n is the number of data (e.g. DBSCAN is $O(nlog(n))$ using kd-tree) [32]. Also, the performance of clustering depends only on the size of the grids which is usually much less than the data objects [31]. Additionally, almost grid-based clustering algorithms are easy to extent parallelization, because each cells are independent when the algorithm detects whether the cell is defined as a cluster or not. Agrawal et al. proposed CLIQUE to extract clusters within subspaces of the dataset using apriori-like technique [36]. Wang et al. present STING which represents a grid-based and density-based approach [35]. Chang et al. proposed Axis-Shifted Grid-Clustering algorithm, which is a dynamic adjustment of the size of the original cells in the grid and reduction of the weakness of borders of cell [3].

Our proposed method to extract area of interests calculates the density of the area which photographers took photographs. We extract clusters as hotspots based on density in a grid space. To calculate a density of each cells in the grid, we use overlaps of the area taken by photographers, calculated by photographic location, orientation, and angle of view of photographs. In this paper, our proposed method adopts the number of overlaps of pseudo triangles at which photographs were taken in each cells to identify a cell is the area of interests or not. The location is a point, but calculated pseudo triangles present an area. Therefore, the amount of data obtained from the pseudo triangles applied to clustering algorithm is more huge, comparing to the approach using photographic location. Therefore, the time complexity of the advantage of the grid-based approach is important to treat huge photographs.

2.2 Extraction of Hotspots Based on Photograph Orientation

According to photographs with a photographic orientation have become more commonly available, photographic orientation is used for extracting hotspots. Lacerda et al. proposed a method for extracting hotspots using photograph orientations [9]. This method calculates the intersections between lines of photographic orientation of many photographs. The intersections are clustered using DBSCAN. Also, Thomee et al. proposed a method for consideration of inaccuracies af-

fecting GPS location measurements [17].

However, those methods to extract hotspots using photographic orientation do not consider the angle of view of photographs. The angle of view is important information which shows an area of user interest. Therefore, we propose a method to extract area of interests considering both photographic orientation and angle of view.

In the related literature, some methods to estimate the photograph orientation have been presented, even for photographs that appear to have no photograph orientation [11], [7]. Our method uses the photographs with photograph orientation to extract area of interests. Therefore, we expect to use the estimated photograph orientation to increase the accuracy of our method.

2.3 Analysis of Extracted Hotspots

Some researchers study the approach to analyze hotspots obtained from large data annotated with various metadata like photographic location.

The method to extract hotspots is used to find or detect geographical characterization. Spyrou et al. proposed a method to understand the underlying semantics of extracted hotspots using user-generated tags [25]. Omori et al. evaluate georeferenced photographs annotated with user-generated tags related to coastlines show actual coastline [37]. Hu et al. proposed a method to understand urban areas from extracted hotspots using user-generated tags, and choice preferable photos based on image similarity of photographs in the hotspot [39].

Also, there are some methods to extract the relationship between a hotspot to another hotspot such as the relationship of photographic subjects and shooting spots. Shirai et al. proposed a method to extract a hotspot using DBSCAN and to calculate the relation of hotspots [14], [42]. To discover a wide area of interest, this approach infers the relation among hotspots based on the photograph location and orientation. Hirota et al. proposed a method to detect and visualize various relationship of hotspots using photographic orientation and social tagging [6]. Those researchers extract some relationships from extracted hotspots.

The area of interests extracted by our proposed method represents photographic subjects at which many people took photographs. In other words, comparing to previous methods to extract hotspots, our methods can extract hotspots reflecting interests of users. Therefore, our approach might contribute researchers to characterize the region and extract relationships using hotspots.

3 PROPOSED METHOD

We propose a method to extract the area of interests using photograph location, orientation, and angle of view obtained from photo-sharing sites. Our approach includes the following steps.

1. For a particular area, we obtain vast numbers of photographs from photo-sharing site.
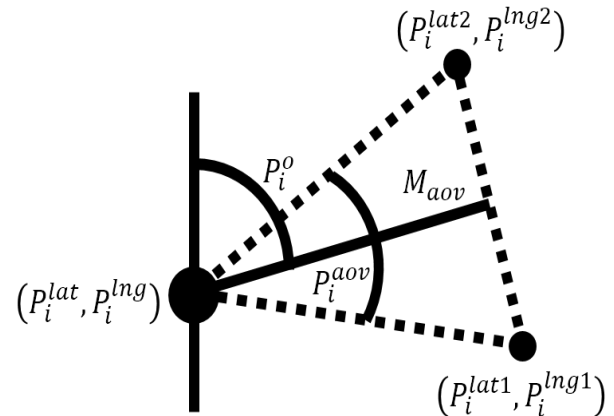
Figure 2: The symbols of pseudo triangle calculated by photographic orientation, location, and angle of view.

2. Generation of a pseudo triangle of a photograph, which represents photograph area which a photographer was taken, based on photographic location, orientation, and angle of view.

3. From photographs which we use to analyze the particular area, we create grid space and cells which the size specified by a user.

4. We count the number of the pseudo triangles in each cell, and define the number is more than the threshold as the area of interest.

We describe details related to the respective steps below.

3.1 Calculation of Pseudo Triangle of a Photograph

We describe calculation of a photograph triangle which represents photograph area using photographic orientation, location and angle of view. Here, Fig. 2 shows the symbols for following equations to calculate the pseudo triangle of a photograph. The pseudo triangle consists photographic location, orientation, and angle of view.

The angle of view is the angular degree of a given scene that is included in the photograph taken with a camera. The angle of view p_i^{aov} of photograph p_i in photographs $P = \{p_1, p_2, ..., p_n\}$ is calculated from focal length p_i^f and the image sensor size p_i^l as follow.

$$p_i^{aov} = 2 * tan^{-1} \left(\frac{p_i^l}{2 * p_i^f} \right) \qquad (1)$$

To calculate the pseudo triangle of a photograph, we detect the three points of the triangle. The triangle of photograph p_i consists of vertex, angle of the vertex, photographic orientation p_i^o, and the other two points. The vertex of the triangle is the photographic location of latitude and longitude obtained from GPSLatitude and GPSLongitude in Exchangeable image file format (Exif). The angle of the vertex is angle of view p_i^{aov} of the photograph p_i. The other two points are calculated based on photographic location and orientation p_i^o, the angle

A cell which overlaps a pseudo triangle of a photograph is defined as its area of interest

A cell which overlaps a pseudo triangle of a photograph is defined as not its area of interest
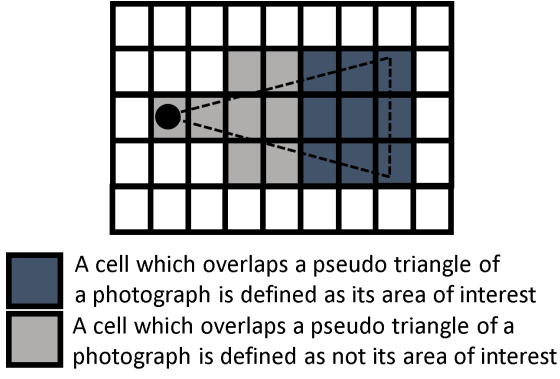
Figure 3: The definition of overlaps of cells and pseudo triangle of a photograph.

of view, and the distance of the photographic subject. We calculate the two points (p_i^{lat1}, p_i^{lng1}) and (p_i^{lat2}, p_i^{lng2}) using following equations.

$$p_i^r = \frac{(p_i^o + p_i^{aov} * 0.5) * \pi}{180} \tag{2}$$

$$d_i^{lat} = M_{aov} * \cos(p_i^r) \tag{3}$$

$$d_i^{lng} = M_{aov} * \sin(p_i^r) \tag{4}$$

$$p_i^{lat1} = p_i^{lat} + d_i^{lat} * \frac{180}{\pi * ER} \tag{5}$$

$$p_i^{lng1} = p_i^{lng} + d_i^{lng} * \frac{180}{\pi * ER * \cos(\frac{p_i^{lat1} * \pi}{180})} \tag{6}$$

Here, ER is radius of earth. Also, M_{aov} shows the parameter how meter distant from latitude p_i^{lat} and longitude p_i^{lng} of photographic location of a photo p_i. (p_i^{lat2}, p_i^{lng2}) are calculated by the same procedure that the direction changes $p_i^o + p_i^{aov} * 0.5$. to $p_i^o - p_i^{aov} * 0.5$.

3.2　Calculation of Grid

To identify places of area of interest which many people have taken in the photograph, we specifically examined the number of overlaps extracted pseudo triangle of photographs. We create a two-dimensional grid which consists square cells. Here, the area which we want to analyze is much wider than the pseudo triangle of one photograph. Therefore, first, we map photographs which have a photograph location to the grid. Also, using the assigned coordinate of the grid, we count the number of the number of extracted pseudo triangle of photographs.

$$y_i = M_{height} - \frac{(p_i^{lat} - Lat_{min}) * M_{height}}{Lat_{max} - Lat_{min}} \tag{7}$$

$$x_i = M_{width} - \frac{(p_i^{lng} - Lng_{min}) * M_{width}}{Lng_{max} - Lng_{min}} \tag{8}$$

Here, Lat_{max}, Lat_{min}, Lng_{max}, and Lng_{min} respectively denote the maximum and minimum values in $\{p_1^{lat}, p_2^{lat}, ..., p_n^{lat}\}$ and $\{p_1^{lng}, p_2^{lng}, ..., p_n^{lng}\}$. Additionally, M_{height} and M_{width} are the number of horizontal and vertical cells. These parameters are decided by how many meters to make one side of

a cell. For example, when the length of height of a cell is $m = 50$ meters, M_{height} are calculated as follow.

$$M_{height} = \frac{h(Lat_{max}, Lat_{min})}{m} \tag{9}$$

Here, $h(Lat_{max}, Lat_{min})$ is Hubeny distance between the Lat_{max} and Lat_{min} (Because these are actually points, either Lng_{min} or Lng_{max} is used for this calculation, but there is almost no difference in the result). M_{width} is calculated by the same procedure.

Consequently, each cells in the obtained grid include a photograph taken in the range.

3.3　Extraction Area of Interest

We discover the area of interest from the obtained cells using the overlaps of pseudo triangle extracted in previous steps. Figure 3 shows the overlapped cells of the pseudo triangle of a photograph. In the figure, the black circle shows the photographic location. Dashed lines of triangle consist of the pseudo triangle of a photograph. Here, the cells filled with light gray or dark gray are overlapped to the pseudo triangle. We detect the overlaps of the dashed line and cells based on photographic location and the vertexes of pseudo triangle of a photograph using Bresenham's line algorithm [43]. In this paper, we use the cells filled with dark gray as the user's interests shown by a photograph. The reason why our approach does not use some cells close to the photographic location is we think those cells might present the shooting spot, not the interests. Although some cell which might be extracted as a shooting spot includes many photographs, and the number of overlaps in such cells may be higher than other cells like not a shooting spot. As a result of the case that we do not eliminate the cells filled with light gray, almost extracted cells are not the area of interests which our approach wants to extra, but shooting spot. Therefore, in this paper, our approach only uses cell filled with dark gray to extract the area of interest.

We classify whether a cell show interests of a photograph by three cases. First, a cell includes the triangle. Second, the triangle includes a cell. Finally, a line segment of the triangle intersects the line segments of a triangle. Additionally, we remove the cells close to the photographic location, from classified cells. The criterion for close cells is the distance based on photographic location and M_{aov}. In this paper, eliminated cells are closer than $0.5 * M_{aov}$ like the cells filled with light gray in Fig. 3.

We apply this procedure to the cells of all photographs and count the number of cells detected as the interests. If the number of photographs in a cell is greater than threshold $minP$, then the cell is classified as an area of interest. Finally, we visualize the extracted area of interest on Google Maps [20].

4　EXPERIMENTS

This section presents a description of experiments conducted using our proposed method. We present and discuss several examples of detection of visualization of area of interest.

(a) Shooting spot   **(b)** Our method   **(c)** Compass clustering
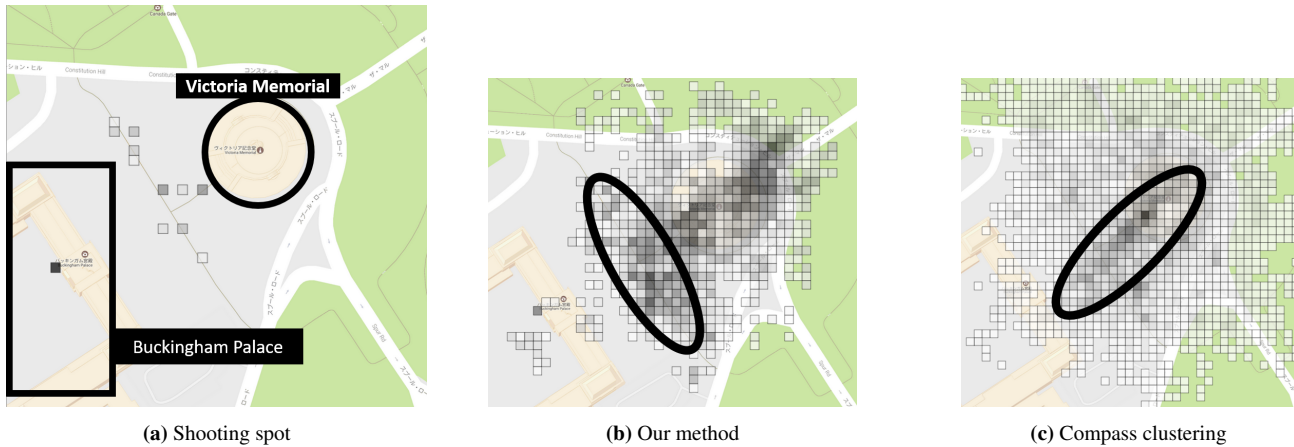
Figure 4: The results obtained from photographs which were taken around Buckingham palace and Victoria Memorial.

4.1 Datasets

We describe the dataset for experiments for visualizing the area of interests. Photographs for experiments are obtained from photographic search results of Flickr. Those photographs have Exif metaadata of latitude (GPSLatitudeRef, GPSLatitude), longitude (GPSLngitudeRef, GSPLongitude), orientation (GPSImgDirection, GPSImgDirectionRef), and focal length. We obtained 5,842,337 photographs taken during 1 January 2005 - 20 20 May 2016 and taken in London.

4.2 Comparison Method

We use compass clustering [9] as comparison method. This clustering method uses the intersections of pseudo orientations of a photograph to extract people's interests. DBSCAN clusters extracted intersections, and the calculated clusters are defined as the area of interests in the method. To simplify comparison between our method and the compass clustering, we change grid-based clustering from the procedure of clustering the intersections. Therefore, we map the intersections into cells of a grid and extract the cells which include the number of photographs than a threshold of $minP$ as the area of interests.

4.3 Visualization of Area of Interests

Figure 4 presents results of hotspots extracted from photographs in the area of Buckingham Palace, using our proposed method, compass clustering, and shooting spots. We used 2,023 photographs taken in the area (latitude: -0.145 - -0.138 and longitude: 51.506 - 51.499). The clustering parameters are set as $minP = 40$, $M_{aov} = 100$ meters, and $m = 5$ meters. Here, in this paper, we set the value of parameters manually with confirming the experimental results. In those figures, the polygon shows the place extracted as a hotspot. In Fig. 4(b) and Fig. 4(c), the more dark color of a polygon from white to black, the cell includes more numbers of the photographic area of photographs. Also, in Fig. 4(a), the more dark color of a polygon from white to black, the more photographs were taken in the area. Also, in those figures, black circle shows the area of Victoria Memorial, and black rectangle shows the area of Buckingham Palace.

Figure 4(a) shows the one shooting spot in Buckingham palace, and eleven shooting spots around Victoria Memorial. The shooting spots include the photographs taken of those subjects. However, although the Victoria Memorial is one of the famous monument and photographic subject, its place is not extracted as shooting spot. The reason is when people may take a photograph of the subject, they take apart from the subject. On the other hand, in Fig. 4(b) and Fig. 4(c), the extracted area of interests shows the more wide area than shooting spots of Fig. 4(a), because those methods use the line of photographic orientations or pseudo triangles.

In result of compass clustering of Fig. 4(c), there are the dark polygons linearly from Victoria Memorial to Buckingham Palace. Because compass clustering extracts the area of interest using the pseudo orientation of photographs, the method tends to extract the area of interests linearly. On the other hand, in the result of our proposed method in Fig. 4(b), there are the black polygons widely in the black ellipse. Here, the gate of Buckingham Palace exists over a wide range in the area of the ellipse. Therefore, many people take photographs of the gate and Buckingham Palace, and our proposed method discover the place as the area of interests in result shown in Fig. 4(b). Our approach uses the angle of view to discover the area of interests to consider the region of the interests. As a result, our proposed method can extract the broad subject as the area of interests.

Next, we show another result in the case that the distance between the area of interests and shooting spots is farther away. Figure 5 presents results of hotspots extracted from photographs around Big Ben and London Eye. There is a Themes river between Big Ben and London Eye. Thus, the distance between those spots is about 500 meters. We used 704 photographs annotated with tags related Big Ben, and taken in the area (latitude: -0.130 - -0.105 and longitude: 51.598 - 51.518). The clustering parameters are set as $minP = 40$, $M_{aov} = 100$ and $m = 10$ meters.

In Fig. 5(a), two shooting spots are extracted around London Eye. Therefore, the result shows there is interest from the place to Big Ben. In Fig. 5(b), and 5(c), both method extracted the area of interests around London Eye and Big Ben. However, the area of interests by compass clustering method

(a) Shooting spot　　　　　　**(b)** Our method　　　　　　**(c)** Compass clustering
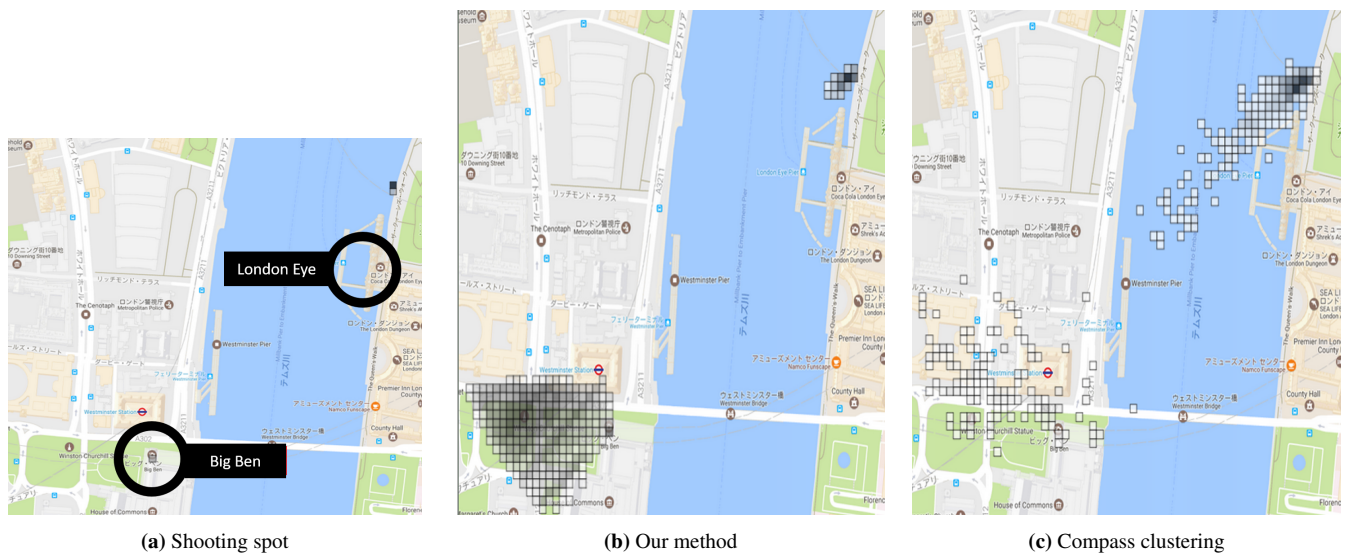
Figure 5: The results obtained from photographs which were taken around Big Ben and London Eye.

is a few that our method around Big Ben, and the compass clustering added heavyweights to the places around London Eye. This reason is that the compass clustering method uses the intersections calculated by the pseudo orientation. In this case, because the area of interests which we want to visualize is far from shooting spots, the points of the intersects is more diverse, and the extraction of the interests is more difficult. On the other hand, because our method calculates the interests using the pseudo triangles which show the users interest, even if the distance is far, our approach can extract overlaps of users interests.

Next, we discuss the parameter M_{aov} of the distance between photographic subject and location of a photograph. In Fig. 5(b), and 5(c), there are some defined cells as the area of interests beyond Big Ben. We assume this reason is the diversification of distance between photographic subject and location in our approach and the compass clustering. Therefore, the photographic areas extracted by our approach have some errors based on the distribution of photographic location.

Figure 6 show the result of area of interest obtained from the same dataset of Fig. 5, when extracting the area of interest using both the cells which close cells from the photographic location (the cells filled with light gray in Fig. 3) and cells which we use to extract area of interest in Section 3.3 (the cells filled with dark gray in Fig. 3). This result shows many photographers took photographs to Big Ben from London Eye. Therefore, the cell with the most significant number of overlaps of pseudo triangles is the area around London Eye. Also, the color of cells changes black into white from London Eye to Big Ben. This shows that the number of the overlaps is decreasing from London Eye to Big Ben. As a result, although fig. 6 shows the result that many photographers took photographs from London Eye and Big Ben, the black cells do not show the area of interests about Big Ben but shooting spots about Big Ben, compared to Fig. 5(b). Therefore, the procedure of excluding the cell which is close to photographic location is important for extracting the accurate area

of interest.

We summarize the visualization result obtained by our proposed method and discuss the performance improvement. Comparing to the area of interest extracted using compass clustering, our proposed method extracts more wide area as the area of interest, shown in Fig. 4. Also, we extract the area of interest around Big Ben, but compass clustering extracted area of interest near London Eye, shown in Fig. 5(c). This reason is intersections of pseudo orientation in compass clustering are concentrated around the shooting spot near London Eye. On the other hand, our proposed method shown in Fig. 5(b) extracted area of interest around Big Ben. This advantage is the pseudo-triangle and the eliminated cells described in Section 3.3. To make extraction of the area of interests more accurate, we should estimate the distance between the photographic location of a photograph and each subject in the photograph.

5　CONCLUSIONS

We proposed a method to extract and visualize the area of interests using photograph metadata of photographic orientation, location, and angle of view obtained from photo-sharing sites. Our approach identifies a cell in grid mapped from photographs into the area of interest or not, using the overlaps of pseudo triangles extracted by the photograph metadata. We presented some examples of results obtained from Flickr using our proposed method. Comparing to the other method to extract the area of interests based on photographic orientation, our proposed method can extract the area of interests at more widely, and it is possible to visualize the contents of the area of interests more importantly.

Future studies will be conducted estimate metadata such as photographic orientation, the distance between the photographic location and the subjects of photograph. Regarding photographic orientation, the applicability of our approach depends on the number of photographs with the metadata and their accuracy. Also, in this paper, we set manually the parameter M_{aov} of distance between subjects of a photograph and
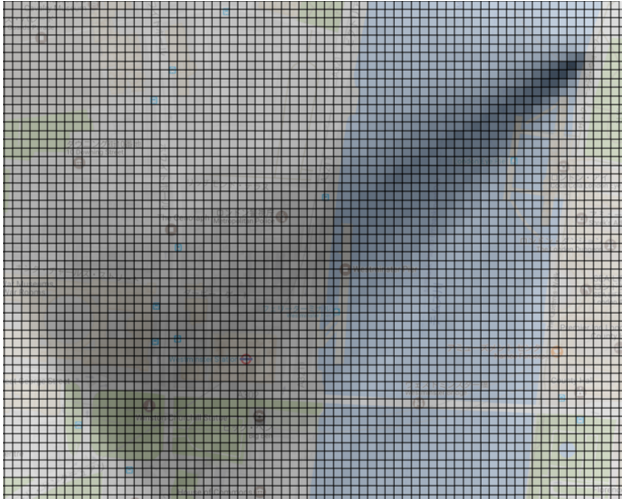
Figure 6: The result of area of interests without excluding the close cells from photographic location (i.e. the result is extracted from light and dark gray cells 3).

photographic location. The parameter M_{aov} depends on the situation of a photographer took a photograph. Therefore, to extract the accurate area of interests extracted by our proposed method, we should set appropriate parameter. Additionally, we will recommend travel routes considering shooting spots and area of interests, because we think that such places which can take photographs around famous landmarks are important for tourism.

ACKNOWLEDGEMENT

REFERENCES

[1] A. Sameer, Y. Furukawa, S Noah, S. Ian, Curless, Brian, Seitz Steven M. and Szeliski, Richard, "Building Rome in a Day", Commun. ACM, vol.54, No.10, pp.105–112 (2012).

[2] S. Ahern, M. Naaman, R. Nair and Yang, Jeannie Hui-l, "World Explorer: Visualizing Aggregate Data from Unstructured Text in Geo-referenced Collections",Proceedings of the 7th ACM/IEEE-CS Joint Conference on Digital Libraries, pages 1–10 (2007).

[3] C. Chang, N. Lin, and Nien-Yi, "An axis-shifted grid-clustering algorithm",Tamkang Journal of Science and Engineering, vol.12, No.2, pp.183–192 (2009).

[4] C. David, B. Lars, H. Daniel, and K. Jon, "Mapping the World's Photos", Proceedings of the 18th International Conference on World Wide Web, pages 761–770 (2009).

[5] M. Ester, H. Kriegel, J. Sander and X. Xu, "A Density-Based Algorithm for Discovering Clusters in Large Spatial Databases with Noise", Proceedings of the Second International Conference on Knowledge Discovery and Data Mining, pages 226–231 (1996).

[6] M. Hirota, M. Shirai, H. Ishikawa and S. Yokoyama, "Detecting Relations of Hotspots Using Geo-tagged Photographs in Social Media Sites", Proceedings of Workshop on Managing and Mining Enriched Geo-Spatial Data, pages 7:1–7:6 (2014).

[7] H. Yen-Ta, C. Kuan-Ting, H. Liang-Chi, H. Winston, and S. Ya-Fan, "Detecting the Directions of Viewing Landmarks for Recommendation by Large-scale User-contributed Photos", Proceedings of the 20th ACM International Conference on Multimedia, pages997–1000 (2012).

[8] K. Slava, M. Florian and K. Daniel, "P-DBSCAN: A Density Based Clustering Algorithm for Exploration and Analysis of Attractive Areas Using Collections of Geo-tagged Photos", Proceedings of the 1st International Conference and Exhibition on Computing for Geospatial Research & Application, pages 38:1 – 38:4 (2010).

[9] L. Yuri Almeida, Feitosa Robson Gonçalves Fechine and Esmeraldo, Guilherme Álvaro Rodrigues Maia and Baptista, Cláudio de Souza and Marinho, Leandro Balby, "Compass Clustering: A New Clustering Method for Detection of Points of Interest Using Personal Collections of Georeferenced and Oriented Photographs", Proceedings of the 18th Brazilian Symposium on Multimedia and the Web, pages281–288 (2012).

[10] L. Xin, W. Changhu, Y. Jiang-Ming, P. Yanwei and Z. Lei, "Photo2Trip: Generating Travel Routes from Geo-tagged Photos for Trip Planning", Proceedings of the International Conference on Multimedia, pages143–152 (2010).

[11] P. Minwoo, L. Jiebo, C. Robert and L. Yanxi, "Beyond GPS: Determining the Camera Viewing Direction of a Geotagged Image", Proceedings of the International Conference on Multimedia, pages 631–634 (2010).

[12] P. Adrian and G. Gregory, "Mining Social Media to Create Personalized Recommendations for Tourist Visits", Proceedings of the 2nd International Conference on Computing for Geospatial Research & Applications, pages37:1–37:6 (2011).

[13] S. Christian and G. Micheal, "Latent Geographic Feature Extraction from Social Media", Proceedings of the 20th International Conference on Advances in Geographic Information Systems, pages149–158 (2012)

[14] M. Shirai, M. Hirota, H. Ishikawa and S. Yokoyama "A Method of Area of Interest and Shooting Spot Detection Using Geo-tagged Photographs", Proceedings of The First ACM SIGSPATIAL International Workshop on Computational Models of Place, pages34:34–34:41 (2013).

[15] S. Noah, G. Rahul, M. Steven and S. Richard, "Finding Paths Through the World's Photos", ACM SIGGRAPH 2008 Papers, vol. 80, No. 2, pp.189–210 (2008).

[16] S. Noah, S. Steven, and S. Richard, "Photo Tourism: Exploring Photo Collections in 3D", ACM SIGGRAPH 2006 Papers, pages 835–846 (2006).

[17] T. Bart, "Localization of Points of Interest from Georeferenced and Oriented Photographs", Proceedings of the

2Nd ACM International Workshop on Geotagging and Its Applications in Multimedia, pages 19–24 (2013).

[18] Z. Haipeng, K. Mohammed, Y. Erkang and C. David J, "Beyond Co-occurrence: Discovering and Visualizing Tag Relationships from Geo-spatial and Temporal Similarities", Proceedings of the Fifth ACM International Conference on Web Search and Data Mining, pages33-42 (2012).

[19] Z. Yan-Tao, Z. Zheng-Jun and C. Tat-Seng, "Research and applications on georeferenced multimedia: a survey", Multimedia Tools Appl, No.1, pp. 77–98 (2011).

[20] Google Maps, https://www.google.co.jp/maps

[21] Flickr, http://www.flickr.com/.

[22] Panoramio, http://www.panoramio.com/.

[23] T. Bart, A. Ioannis amd S. David A, "Finding Social Points of Interest from Georeferenced and Oriented Online Photographs", ACM Trans. Multimedia Comput. Commun. Appl., vol. 12, No. 2, pp. 36:1–36:23 (2016).

[24] S. Jieming, M. Nikos, W. Dingming and C. David W, "Density-based Place Clustering in Geo-social Networks", Proceedings of the 2014 ACM SIGMOD International Conference on Management of Data, pages99–110 (2014).

[25] S. Evaggelos, K. Michalis, C. Vasileios, P. Apostolos and M. Phivos, "A Geo-Clustering Approach for the Detection of Areas-of-Interest and Their Underlying Semantics", Algorithms, vol. 10, No.1, pp.35 (2017).

[26] W. Yang and C. Liangliang, "Discovering latent clusters from geotagged beach images", International Conference on Multimedia Modeling, pages133–142 (2013).

[27] R. Tye, G. Nathaniel and N. Mor, "Towards Automatic Extraction of Event and Place Semantics from Flickr Tags", Proceedings of the 30th Annual International ACM SIGIR Conference on Research and Development in Information Retrieval, pages103–110 (2007).

[28] F. Laura, R. Alberto, M. Marco and Z. Franco, "Extracting Urban Patterns from Location-based Social Networks", Proceedings of the 3rd ACM SIGSPATIAL International Workshop on Location-Based Social Networks, pages 9–16 (2011).

[29] V. Olivier, S. Steven and D. Bart, "Finding Locations of Flickr Resources Using Language Models and Similarity Search", Proceedings of the 1st ACM International Conference on Multimedia Retrieval, pages48:1–48:8 (2011).

[30] H. Livia and P. Ross, "Exploring place through user-generated content: Using Flickr tags to describe city cores", Journal of Spatial Information Science, vol.2010, pp.21–48 (2010).

[31] P. Monali and V. Tanvi, "Survey on different grid based clustering algorithms", Int J Adv Res Comput Sci Manag Stud, vol.2, No.2 (2014).

[32] M. Amandeep Kaur and K. Navneet, "Survey paper on clustering techniques", IJSETR, vol.2, No.4, pp.803–6 (2013).

[33] S. Jörg, E. Martin, K. Hans-Peter and X. Xiaowei, "Density-Based Clustering in Spatial Databases: The Algorithm GDBSCAN and Its Applications", Data Min-

ing and Knowledge Discovery, vol.2, No.2, pp. 169–194 (1998),

[34] A. Mihael, B. Markus, K. Hans-Peter and S. Jörg, "OPTICS: Ordering Points to Identify the Clustering Structure", Proceedings of the 1999 ACM SIGMOD International Conference on Management of Data, pages 49–60 (1999).

[35] W. Wei, Y. Jiong and M. Richard R, "STING: A Statistical Information Grid Approach to Spatial Data Mining", Proceedings of the 23rd International Conference on Very Large Data Bases, pages186–195 (1997).

[36] A. Rakesh, G. Johannes, G. Dimitrios and R. Prabhakar, "Automatic Subspace Clustering of High Dimensional Data for Data Mining Applications", Proceedings of the 1998 ACM SIGMOD International Conference on Management of Data, pages94–105 (1998).

[37] M. Omori, M. Hirota, H. Ishikawa and S. Yokoyama, "Can Geo-tags on Flickr Draw Coastlines?", Proceedings of the 22nd ACM SIGSPATIAL International Conference on Advances in Geographic Information Systems, pages425–428 (2014).

[38] V. Steven, S. Steven and D. Bart, "Discovering and Characterizing Places of Interest Using Flickr and Twitter", Int. J. Semant. Web Inf. Syst., vol.9, No.3, pp.77–104 (2013).

[39] Y. Hu, S. Gao, K. Janowicz, B. Yu, W. Li and S. Prasad, "Extracting and understanding urban areas of interest using geotagged photos", Computers, Environment and Urban Systems, vol.54, pp.240–254 (2015).

[40] D. Comaniciu, P. Meer, "Mean shift: a robust approach toward feature space analysis", IEEE Transactions on Pattern Analysis and Machine Intelligence, vol.24, No.5, pp.603–619 (2002).

[41] Y. Yiyang, G. Zhiguo and L. Hou, "Identifying Points of Interest by Self-tuning Clustering", Proceedings of the 34th International ACM SIGIR Conference on Research and Development in Information Retrieval, pages 883–892 (2011).

[42] M. Shirai, M. Hirota, S. Yokoyama, N. Fukuta and H. Ishikawa, "Discovering Multiple HotSpots Using Geotagged Photographs", Proceedings of the 20th International Conference on Advances in Geographic Information Systems, pages490–493 (2012).

[43] B. Jack E, "Algorithm for computer control of a digital plotter", IBM Systems journal, vol.4 No.1, pp.25–30 (1965).

Masaharu Hirota received B.E, M.E, and Ph.D degree of Informatics from Shizuoka University. After working for Department of Information Engineering, National Institute of Technology, Oita College, he has been working as associate professor in Faculty of Informatics, Okayama University of Science from April, 2017. His research interests include data engineering, web mining, geographic information, and visualization. He is a member of ACM, STI, DBSJ, and IPSJ.

Masaki Endo earned a B.E. degree from Polytechnic University, Tokyo and graduated from the course of Electrical Engineering and Computer Science, Graduate School of Engineering Polytechnic University. He received an M.E. degree from NIAD-UE, Tokyo. He earned a Ph.D. Degree in Engineering from Tokyo Metropolitan University in 2016. He is currently an Assistant Professor of Polytechnic University, Tokyo. His research interests include web services and web mining. He is also a member of DBSJ, NPO STI, IPSJ, and IEICE.

Daiju Kato is product quality specialist at WingArc1st.Inc. and doctor course student in Tokyo Metropolitan University. His research area is software quality assurance, software testing and data engineering. He is member of JSQC and Society for Serviceology.

Ishikawa Hiroshi received the B.S. and Ph.D degrees in Information Science from the University of Tokyo. After working for Fujitsu Laboratories and being a full professor of Shizuoka University, he is now a full professor of Tokyo Metropolitan University from April, 2013. His research interests include database, data mining, and social big data. He has published actively in international, refereed journals and conferences, such as ACM TODS, IEEE TKDE, VLDB, IEEE ICDE, and ACM SIGSPATIAL. He has authored some books, Social Big Data Mining (CRC Press). He is fellows of IPSJ and IEICE and members of ACM and IEEE.

Regular Paper

BLE Beacon's Defect Detection Method Based on Room Model of BLE and Wi-Fi

Shota Ikeda[†], Fumitaka Naruse [‡], and Katsuhiko Kaji[‡]

[†]Graduate School of Business Administration and Computer Science, Aichi Institute of Technology, Japan
[‡]Department of Information Science, Aichi Institute of Technology, Japan
{b17703bb, k14092kk, kaji}@aitech.ac.jp

Abstract - In this research, we propose a defect-detection method for a Bluetooth Low Energy (BLE) beacon. The types of defect are breakdown, battery exhaustion, removal and relocation. To detect such defects, we create a BLE model and Wi-Fi model for each room. The BLE model and Wi-Fi model consist of probabilities of observation of each beacon's radio information. By comparing the newly acquired BLE radio information and Wi-Fi radio information with the BLE/Wi-Fi room model, it is possible to detect the problem occurring in the beacon. As a proposed method, we compare the room model with the radio-wave information of the acquired BLE and Wi-Fi, and detect the beacon defect automatically. We conducted indoor experiments and beacon defect-detection experiments using the proposed method. In the room estimation experiment, the accuracy of estimation at BLE with the optimal boundary value was 86%, and the estimation accuracy at Wi-Fi was 95%. In beacon defect-detection experiments, the correct answer rate for defect detection was 94%. However, when the beacon disappeared from a room, the detection accuracy was 35%, which was less than half.

Keywords: BLE beacon, fingerprint, room estimation, defect detection, Wi-Fi

1 INTRODUCTION

BLE beacons (from here on, simply 'beacons') are increasingly used for services in public facilities such as indoor location estimation, room estimation, attendance management, distribution of coupons, mountaineer distress prevention, and checkpoints of electronic stamp rallies [1]–[4]. To estimate the position of a room in room estimation, one to several beacons are installed in each room. Also, there are many methods of installing beacons at a fixed distance, and they are used for indoor management and recording of walking routes [5], [6]. They are used to distribute coupons to the smartphones of people who pass in front of a store [7]. For mountaineering safety, climbers can bring beacons that sound an alert if anyone strays too far from the group. In electronic stamp rallies, beacons are installed at checkpoints. When a smartphone is close to the checkpoint's beacon, the user can press the stamp on the smartphone application [8], [9].

Because beacons are small and easy to carry, it is difficult to manage many beacons simultaneously. Beacons run on batteries whose lifetime is from about six months to two years. Thus, when dealing with many beacons, we have to check every one to figure out which has run out of batteries. Also,

beacons are small, have the same shape, and are easy to carry. Therefore, someone can move them accidentally, or they can be miss installed.

When the target environment is small, usually the administrator of the environment can easily manage the small number of beacons because it is easy to grasp what kind of defect is occurring in which beacon and respond quickly.

In a large-scale environment with many beacons such as a university or electronic stamp rally at a large park, the administrator must collectively manage the system, and it is unrealistic to check beacons for failure one by one.

In this research, we generate a BLE/Wi-Fi-based room model to estimate defects such as battery outage, malfunction, removal, and relocation. The BLE model and the Wi-Fi model consist of probabilities of observation of signal information for each room. When a new BLE/Wi-Fi radio wave observation is acquired, the system compares the obtained radio wave information with each room model, and estimates the room from which the radio waves were acquired. After that, the system compares the estimated room model with the acquired radio wave information and finds the beacon defect.

Battery-powered beacons are mostly used, so the batteries run out during long-term operation. Also, since beacons are small and have a shape that is difficult to fix to a wall, there is the possibility of them being moved. Additionally, in order to manage many beacons, there are cases where beacons are mistakenly installed in the wrong room. Because beacons only transmit BLE radio waves, they cannot communicate with each other. Therefore, it is impossible to confirm problems between beacons.

Using the proposed method, the administrator does not have to undertake the impractical task of checking each beacon individually.

The rest of this paper is structured as follows. In Section 2, we explain related research. Section 3 describes our beacon defect detection method. Section 4 describes experiments using the proposed method. Section 5 summarizes and discusses future issues.

2 RELATED RESEARCH

Wireless LAN, beacons, built-in sensors of smart phones, etc. are often used for indoor position estimation and room estimation research. However, there are few studies on detecting activity or defects of beacons for terminal management.

There is research on the behavior monitoring of BLE beacons using participatory sensing. In Asahi's method [8], the

beacon is used as a check point of an electronic stamp rally. When the smartphone terminal that introduced the application receives radio waves, beacon information and time data are sent to the server. When monitoring the information transmitted to the server, the data continuously transmitted may be interrupted in some cases. Since the transmission of data suddenly stops, it is a method that grasps the activity state of the beacon. This method is considered to be effective as beacon management during service operation. However, if the beacon installed as a checkpoint is moved, or if it is installed at a place where people do not always go, it cannot be determined whether the beacon is running or not. Also, there is a possibility that some time lag may occur between a beacon sending information, and that information being confirmed. Additionally, even if a beacon is moved to an unexpected place, when someone brings a smartphone within range of that beacon, the method confirms that the beacon is normal.

When estimating position using campus LAN, it is necessary to measure the radio wave intensity of Wi-Fi for each position. When using the wireless access point to estimate the position as in Dhruv's method [10], it is necessary to determine the observation position of the radio wave intensity considering the base station. In contrast, our method creates Wi-Fi and BLE fingerprints. Instead of a fingerprint for each location, it creates a fingerprint for each room based on the measured data. When you create a fingerprint for each room, you cannot figure out where you are in the room. However, it becomes easy to grasp whether or not you are in the room. When indoor position estimation using radio field strength of a BLE device is carried out, radio waves of BLE are weaker than Wi-Fi.

Kajioka's method involving indoor positioning using BLE radio intensity [11] targets small classrooms. Therefore, only one beacon is placed for each room. Even though radio waves may be weak, the beacon's radio waves could be received everywhere in small rooms. It is considered that the possibility of a radio wave not reaching an estimation device is low. However, we also assume a lecture room and a large lecture room compared to Kajioka's research. Therefore, there is a possibility that some places cannot be reached depending on location. Therefore, we should install multiple beacons if a room is so large.

3 BEACON DEFECT DETECTION METHOD USING WI-FI AND BLE OBSERVATION

In this research, we generate a Wi-Fi model and BLE model for each room, and detect defects such as battery outage or breakdown or relocation of a beacon. An outline of this method is shown in Fig. 1. In scene 1, when comparing the observed data with the room model of each room, it can be estimated that the user is at room α from the Wi-Fi model. However, the BLE signal is not received from beacon A. Therefore, beacon A is thought to have experienced a defect such as battery exhaustion or relocation. In scene 2, when comparing the model of room α with the observed data, the existence of beacon B can be confirmed. Since there is no beacon B in the room
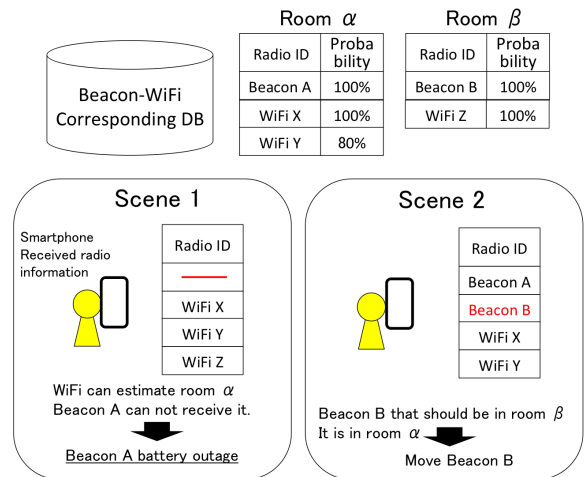
Figure 1: Outline of proposed method

model of room α, there is a high possibility that beacon B was moved from room β to room α.

By using this method, operation check of a beacon can be done automatically. It is not necessary to periodically check the operation of each beacon. It is also considered that defects such as in Fig. 1 can be detected during operation. By doing this, it is possible to deal with the beacons which the defects have occurred.

3.1 System Overview

An overview of the system is shown in Fig. 2. This method is introduced together with room estimation-based applications such as attendance-management applications and coupon-delivery applications. BLE/Wi-Fi observation data is acquired for users who frequently use these applications. The timing to acquire the data is when the BLE is received. Also, the user here is not a system manager, but general users who use the application on a daily basis. In the normal state, when it receives BLE radio waves, it communicates with the room estimation server and receives room information. There is a room recognition library as the foundation of location information service. Normally, in the library, room recognition is performed using only BLE in order to judge the occupancy situation necessary for location information service. BLE models of all rooms are synchronized from maintenance server to room estimation server, and regular room estimation is done by using BLE model. Sometimes, when receiving BLE, it also receives Wi-Fi and sends two pieces of observed information to the maintenance server. Please note that the BLE/Wi-Fi observation task is not explicit. Observed BLE/Wi-Fi can be uploaded to the management database without the user's awareness. When observation information is uploaded, the maintenance server estimates the beacon defect based on the received radio wave information. The server detects a problem with the BLE beacon using both the BLE model and the Wi-Fi model. When a problem is found in the beacon, information on the room and the beacon in which the problem occurred is presented to the manager. Then, the
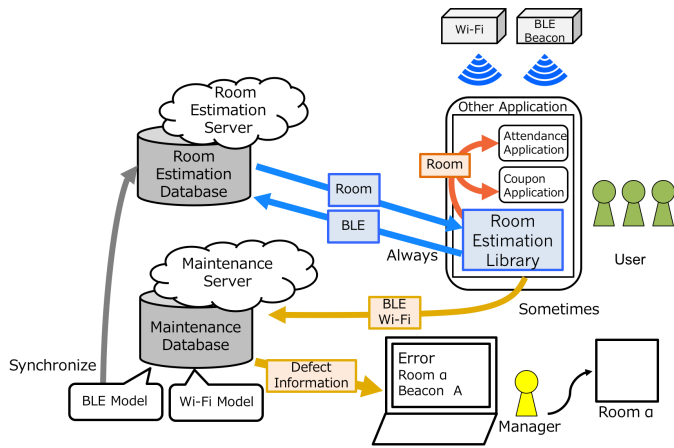
Figure 2: System overview
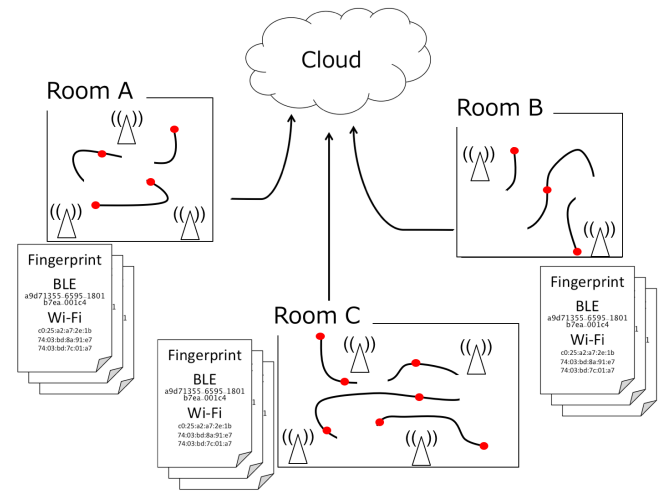
Figure 3: Collecting fingerprint

Table 1: Characteristics of beacon and Wi-Fi router

	BLE beacon	Wi-Fi router
Installation cost	◯	△
Installation place	◯	△
Driving time	△	◯
Detection range	△	◯
Power consumption	◯	△

manager can see the defect information and go to the place to correct the problem.

In fact, you can estimate a room without using beacons if you use Wi-Fi. A comparison of the characteristics of Wi-Fi routers and beacons is shown in Table 1. We decided to utilize beacons instead of Wi-Fi routers based on that. Beacons are inexpensive to install and many can be placed in the same location. Also, since they are mostly battery-powered, installation is possible without being restricted by electrical access. Because beacons use BLE, they operate with power saving, and the transmission range of radio waves is narrow. However, the lifespan is as short as one to two years. Wi-Fi routers are expensive to install and not suitable for installation in many rooms. Since they need a power supply to operate, installation locations are limited. However, since the possibility of interrupting operation is low, reliability is high and radio waves can be transmitted over a wide range.

In this study, we are targeting all the rooms of one building or one campus such as a university, so it is considered that beacons are suitable for installing in each room because they are cheap and easy to install. Basically, Wi-Fi routers are used to access the Internet, so it is not realistic to install them in a room that is not used much. If we estimate the narrow range of a room, it is considered that a narrower range is better than transmitting a radio wave over a wide range. As such, beacons are considered suitable.

3.2 Features of This Method

In this method, we generate a fingerprint for each room rather than a fingerprint for each measured position [12]–[15],

which is being done in many position estimation studies. For each room, not for each location, no matter the detailed location of the observation point. Observe each room rather than location. Then, it is estimated as that room which is regardless of where in the room. Therefore, room estimation is easy. Also, compared to the method that requires observation of detailed positions, the number of observations of radio-wave fingerprints for information can be reduced. This leads to cost reduction. Furthermore, there is no need to clearly decide when to measure radio information. There is the advantage that it is sufficient to observe data everywhere in the room.

The reason for combining Wi-Fi and BLE is to use Wi-Fi to detect a beacon defect when it occurs. It also plays the role of room estimation. When estimating a room by installing a single beacon in a small room such as a small classroom or a laboratory, it is impossible to estimate a room if a beacon fails or a beacon is taken out. Also, in the case of breakdown, the beacon will be repaired if replaced. However, when it is taken out, it is necessary to search for a beacon terminal.

Data collection and modeling of this method are shown in Fig. 3 and Fig. 4. In this method, the system knows all beacon ID's and their room placements. In the case of a small room, beacon radio waves can be acquired anywhere in the room. In the case of a large room, radio waves of the arranged beacon may not be acquired in some cases. If data cannot be acquired continuously, it could be erroneously detected that a defect has occurred in the beacon. Therefore, in our assumption, several beacons are placed in a large room to avoid this problem. The system collects Wi-Fi and BLE radio wave information to estimate a room, and integrates the collected Wi-Fi and data for each BLE. We create a Wi-Fi model and a BLE model for each room as in Fig. 4.

During operation, we gather BLE/Wi-Fi observation data from various people that use room estimation-based applications such as automatic attendance systems and stamp rally games. Basically, BLE data is observed when entering a room as in Fig. 3. The system also observes Wi-Fi data at regular intervals and compares the observed BLE list with the BLE

Fingerprint group   Percentage of visible radio
waves in specific room

BLE A	BLE A
BLE B	BLE C
Wi-Fi X	Wi-Fi X
Wi-Fi Y	Wi-Fi Z
Wi-Fi Z	

RoomA

BLE A	BLE A
BLE C	BLE B
Wi-Fi X	BLE C
Wi-Fi Z	Wi-Fi Y
	Wi-Fi Z

BLE model	
Beacon A	100%
Beacon B	50%
Beacon C	75%
Wi-Fi model	
Wi-Fi X	75%
Wi-Fi Y	50%
Wi-Fi Z	100%

Room model
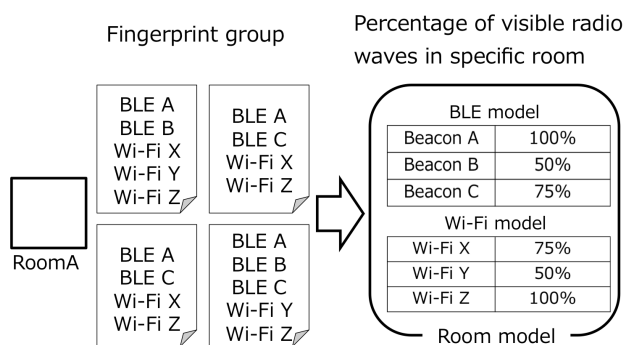
Figure 4: Model creation method

model in every room and estimates the room. Room information is sent after room estimation is done. The system compares the Wi-Fi list observed every fixed period with the Wi-Fi model of every room and estimates the room. The system then compares the observed Wi-Fi list with the Wi-Fi model of the room.

Basically, room estimation for room estimation-based applications is performed using BLE data, but room estimation is performed simultaneously with BLE using Wi-Fi data at regular intervals for detecting beacon defects. We believe that estimation of beacon movement, malfunction, battery exhaustion, etc. will be possible. In addition, when room estimation is performed normally, each model is updated using the observed Wi-Fi and BLE data.

In this method, the system only knows the initial placement room of the beacons. We do not consider it to be a defect situation if a beacon is slightly moved in the same room because the beacon is still in the correct room. However, the BLE signal model for the room should be updated in such a situation. We assume that participatory sensing is a suitable method to update the BLE/Wi-Fi signal model for each room. In operation of room-estimation applications, a user's smartphone uploads BLE/Wi-Fi observation information automatically. By using the collected observation information, the BLE/Wi-Fi model can be updated.

3.3   Data Collection and Assumption

In the proposed method, the fingerprint for Wi-Fi and BLE is collected in advance to generate the BLE/Wi-Fi model for each room. As a premise, smartphones are used to collect data. Observation data at the time of preliminary collection are gathered with the correct room name known. In data collection, we walk around in each room, and record radio observation information of BLE and Wi-Fi at 10-second intervals. In a general Wi-Fi fingerprint collecting method, radio waves obtained while stationary for several seconds are regarded as the fingerprint at that position. On the other hand, in the proposed method, we model the radio-wave environment of each room. Therefore, radio-wave information of the whole room

is necessary. BLE and Wi-Fi radio waves are affected by people and objects, and they decay as distance increases. Therefore, it is insufficient to observe only one point in the room, especially in a large room. We walk around the room and collect fingerprints in various places in the room.

At the time of data collection, we assume that beacons have already been installed in each room. In addition, many kinds of BLE devices have been released in recent years. To avoid confusion, only beacons with a specific UUID (ID that can be set in the beacon) are targets for data collection. The transmission interval of the beacon device used was 300 ms, and the transmission strength was set to -4 dBm.

Data collection is conducted by participatory sensing, and when a user with a smartphone enters a room, observation is assumed simultaneously with room estimation. Basically, the smartphone collects BLE data, but also collects Wi-Fi data at regular intervals. We integrate the collected Wi-Fi of the room and data of each BLE, create a Wi-Fi model and BLE model for each room, and make a room model.

3.4   BLE/Wi-Fi Modeling For Each Room

We create Wi-Fi and BLE models for each room based on the data observed as in Fig. 4 for room estimation. In the proposed method, for the radio waves observed in the room, the probability of observing the radio waves is calculated, and the Wi-Fi model and BLE model are generated. However, for Wi-Fi, radio wave broadcast distance is greater than that of BLE. Therefore, it is limited to those observed above a certain received signal strength. The main reason for using such a simple model is to ease implementation and reduce calculation cost.

Also, for both the Wi-Fi model and BLE model, radio waves with observation probability of less than 50% are not included in the model. Room estimation is performed based on the observation probability of each radio wave. However, if extremely low radio-wave information is included at that time, the probability of room estimation is considered to be low. This is because radio-wave information, which is not frequently observed, is used for room estimation.

3.5   Room Estimation

Room estimation during operation is explained here. We compare the data observed at a certain timing, the list of Wi-Fi and BLE in each room built in advance, the BLE model and the Wi-Fi model, and estimate the room. We focus on room estimation by the BLE model, but that using the Wi-Fi model is done in the same way.

We use only the BLE model for room estimation for location-based services such as attendance management systems. We use the BLE model and the Wi-Fi model for maintenance as to whether the BLE beacon is installed properly.

Let O_b be the set of BLE radio waves contained in observational data O. At this time, the probability $p(r)$ existing in a room r is calculated as follows. Here, we denote the observed probability of radio wave a in room r as $p(a|r)$ and the set of radio waves contained in the BLE model of room r as M_b^r. First, we obtain the set of radio waves common to O_b and

M_b^r as $O_b \cap M_b^r$. Also, we obtain a set of radio waves that are included in M_b^r and not included in O_b as $M_b^r - (O_b \cap M_b^r)$. Next, we obtain the probability that the radio waves of the set element can be observed in room r as follows.

$$p(r) = \prod p(a|r) \times \prod (1 - p(b|r))$$

where

$$a \in O_b \cap M_b^r, b \in M_b^r - (O_b \cap M_b^r).$$

Next, we will explain room estimation with the Wi-Fi model. It is the same as room estimation using the BLE model just by changing the sign of the calculation.

Let O_w be the set of Wi-Fi radio waves contained in observational data O. At this time, the probability $p(r)$ existing in a room r is calculated as follows. Here, we denote the observed probability of radio wave a in room r as $p(a|r)$ and the set of radio waves contained in the Wi-Fi model of room r as M_w^r. First, we obtain the set of radio waves common to O_w and M_w^r as $O_w \cap M_w^r$. Also, we obtain a set of radio waves that are included in M_w^r and not included in O_w as $M_w^r - (O_w \cap M_w^r)$. Next, we obtain the probability that the radio waves of the set element can be observed in room r as follows.

$$p(r) = \prod p(a|r) \times \prod (1 - p(b|r))$$

where

$$a \in O_w \cap M_w^r, w \in M_w^r - (O_w \cap M_w^r).$$

Comparing the observation data with any room model as described above, the probability of being a specific room is required. Let the room with the highest probability be the room where the smartphone is currently.

3.6 Beacon Defect Detection

Based on the results of BLE room estimation and Wi-Fi room estimation, we compare BLE radio wave list O_b with the BLE model of the estimated room and detect the defect of a BLE beacon. The malfunction of a BLE beacon is such that radio waves are not transmitted due to battery exhaustion or breakdown, or it has been taken out of the room. For these defects, we will discover two types of inconsistencies: "Should not be observable" and "Observable but are not". Then, we perform defect analysis.

As a precondition, R_b is the room estimated by the BLE model. R_w is the room estimated by the Wi-Fi model. O_b is the set of BLE beacons received at a given observation. M_b^R is the set of BLE beacons included in the BLE model in room R.

First, we will show the algorithm for finding the beacon set Emh (mh means "move here" from somewhere), which is supposed to be unobservable. What can be found with this pattern is that the beacon was moved to a room observed from some room.

Suppose the room estimate R_b based on the BLE model is correct. The beacon set that is supposed to be impossible to observe can be obtained as follows.

$$E_b^{mh} = O_b - (M_b^{R_b} \cap O_b)$$

On the other hand, suppose that the room estimate R_w based on the Wi-Fi model is correct. The beacon set that is supposed to be impossible to observe can be obtained as follows.

$$E_w^{mh} = O_b - (M_b^{R_w} \cap O_b)$$

Here, if R_b and R_w are different, elements of E_b^{mh} and E_w^{mh} are also different. In that case, their union is regarded as a candidate for a problem.

$$E^{mh} = E_b^{mh} \cup E_w^{mh}$$

Next, we show an algorithm to examine the beacon set E^{mt}(mt means "move to somewhere"), which is supposed to be observed but is not observed. What we can discover with this pattern is a malfunction, a battery exhaustion, or that the beacon has been moved out of the observed room.

Suppose the room estimate R_b based on the BLE model is correct. A beacon set that is supposed to be observed but is not observed is obtained as follows.

$$E_b^{mt} = M_b - (M_b^{R_b} \cap O_b)$$

On the other hand, suppose that the room estimate R_w based on the Wi-Fi model is correct. A beacon set that is supposed to be observed but is not observed is obtained as follows.

$$E_w^{mt} = M_b - (M_b^{R_w} \cap O_b)$$

Here, if R_b and R_w are different, elements of E_b^{mt} and E_w^{mt} are also different. In that case, their union is regarded as a candidate for a problem.

$$E^{mt} = E_b^{mt} \cup E_w^{mt}$$

3.7 Comparison With Other Methods

As related research, compare Asahi's method, described in Section 2, with our method. Table 2 compares attributes of the two methods. In Asahi's method, a beacon is arranged as a checkpoint of a stamp rally. Therefore, it is necessary to transmit data at every checkpoint. Since it is sufficient to transmit only the BLE data, it is considered that the power consumption does not increase very much. However, with this method, it is necessary to transmit Wi-Fi and BLE data when entering the room. Since entrance/exit is repeatedly performed, it is thought that power consumption will increase.

With regard to estimation of defects, Asahi's method does not transmit data unless a person passes near a beacon. Furthermore, we cannot observe data. Also, defect cannot be detected if data cannot be observed. However, in our method, data observation is done at entry. Except for rooms that are not used much, we believe that we can respond quickly to a problem with beacons.

Regarding the type of defect, Asahi's method can only detect defects such as a beacon's battery outage. Also, if a beacon is taken out, you do not know where it has gone. In our

Table 2: Comparison of methods

	Asahi's method [8]	This method
Power consumption	○	△
Immediate nature of defect detection	△	○
Types of defects	△	○

method, a room model is created, and observed data are compared. As a result, in addition to a defect of the beacon, movement such as replacement can be detected.

4 ROOM ESTIMATION AND BEACON DEFECT DETECTION EXPERIMENT

By examining the room-estimation method conducted in Section 3, we can verify the accuracy of room estimation. We also conducted experiments as to whether beacon defects could be detected. If the accuracy of room estimation obtained by experiment is low, there is a possibility that estimation of beacon defects may be affected.

As the first experiment, after creating the BLE/Wi-Fi model, we observe the Wi-Fi and BLE data in each room and obtain the accuracy of room estimation. Since beacon radio waves are weaker than Wi-Fi, it can be considered observable in the room and still not be observed. Therefore, we observe data at various places in the room. It is considered that room estimation is possible with a high probability if the room is isolated. However, it is considered difficult if it is possible to observe radio waves of the same Wi-Fi or beacon, such as in a room next door. In addition, it is thought that the probability of room estimation will be low if all the beacons with low radio field intensity are used. Then, estimation of a beacon defect is affected. Therefore, the boundary value of the radio field intensity is also found.

As a second experiment, we will detect malfunctions assuming beacon movement, defect, etc. We anticipate the following kinds of defect: one cannot observe the beacon in the room; the beacon in the room has malfunctioned; a beacon that should not be observable originally is detected; and a beacon installed in one room has been moved to another room. As a result, we believe that by comparison with BLE/Wi-Fi observation and the BLE/Wi-Fi model of each room, beacon movement and malfunction can be detected.

The factors that affect detection accuracy are considered to be the size of the room, location of the room, and number of beacons.

These factors, along with multiple potential defects, may combine variously to affect detection accuracy.

4.1 Experiment Setting

As the experimental setting, data collection is done in each room using a smartphone as in Section 3. The room used in the experiment is shown in Fig. 5. One Wi-Fi access point is installed in each room. Data collection takes place everywhere in the room.

The beacon arrangements for each room are shown in Fig. 6. Everywhere in the room at least one beacon's signal can be
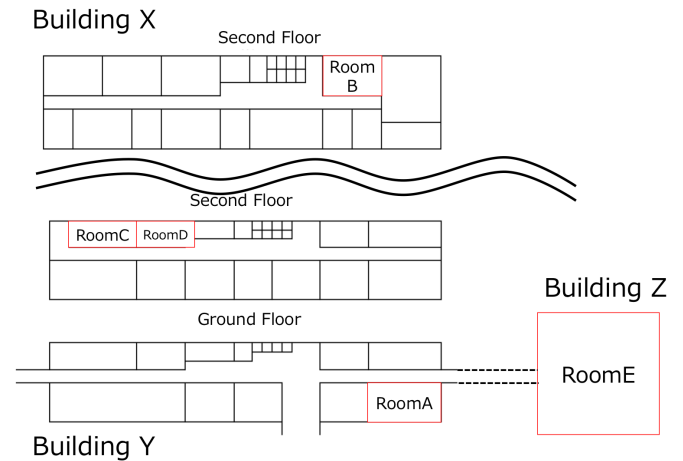
Figure 5: Floor map
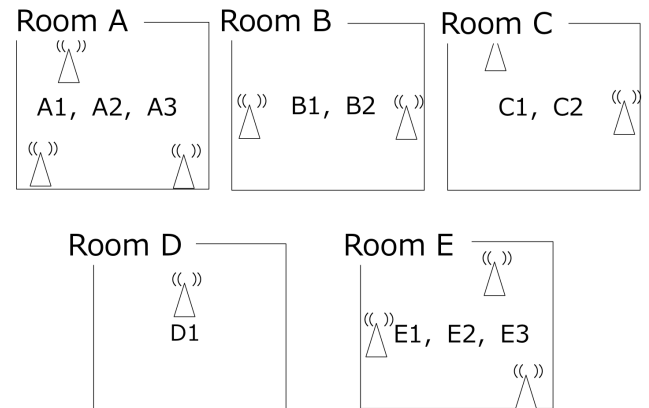
Figure 6: Beacon arrangement diagram

received. All UUIDs are unified. In room A, three beacons are installed in different corners of the room, three in total, and it is apart from the other rooms. In room B, two beacons are installed on opposite walls; and room B is in a different building from the other rooms and thus furthest away. In room C, two beacons are installed, and it is next to room D. In room D, one beacon is installed in the center. Room E is a large lecture room and has beacons installed in three places: entrance 1, entrance 2, and next to the central pillar. Observe BLE and Wi-Fi while walking through the room. Also BLE and Wi-Fi data are acquired 10 times in each room, 50 times in total. The quality of room model will be better when observation time becomes long. Also, the accuracy of room estimation will be approved. However, we decided the number of observation per room is 10 times, because the purpose of the experiment is to confirm the ability of defect detection in the experiment. Actually, the setting of the number of observation per room is rigid condition.

Table 3: Room estimation result

Room estimation	-50dBm		-75dBm		-90dBm	
	BLE	Wi-Fi	BLE	Wi-Fi	BLE	Wi-Fi
RoomA	100%	100%	100%	100%	100%	100%
RoomB	100%	100%	100%	100%	100%	100%
RoomC	100%	70%	100%	80%	100%	100%
RoomD	30%	100%	40%	100%	30%	80%
RoomE	100%	100%	100%	100%	100%	100%
Overall probability	86%	94%	88%	96%	86%	96%

4.2 Room Estimation Experiment

In the room-estimation experiment, we used the Wi-Fi and BLE observation data and experimented on how accurately room estimation could be estimated. We compared the observed data with the model created in Section 3. If the accuracy of room estimation is low, it is thought that estimation of beacon defects will be affected. Also, if all the base-station information is used, there is a possibility that the probability of room estimation will be low. Since there is a possibility that the experiments to be performed next may be affected, the boundary value is also examined. Boundary values of -50 dBm, -75 dBm, and -90 dBm were used for room estimation. Experimental results are shown in Table 3.

For room A, the room estimate for BLE was 100% at any boundary value of the radio field strength. Room B was 100% different at any boundary value because it is in a different building from the other rooms. For room C, the estimate for BLE was 100%, but for Wi-Fi the estimate at -50 dBm was 70% and the estimate at -75 dBm was 80%. For room D, BLE estimates were less than 40% at any boundary value; estimate for Wi-Fi at -90 dBm was 80% and others were 100%. Room E was 100% in BLE and Wi-Fi estimates.

From the experimental results, we could estimate a room with high probability except for ones with a room next door. However, in rooms next to each other, we could observe the BLE and Wi-Fi radio waves from either room. Therefore, it is considered difficult to estimate only by whether the base station can be observed. Moreover, accuracy is high when room estimation is performed at -75 dBm from the experimental result. Therefore, the boundary value considered to be suitable for defect detection is -75 dBm.

As a result, the influence of the number of beacons and the size of the room is small. However, when the position of the room is close, the beacon radio waves can be acquired, so the detection accuracy is low.

4.3 Beacon Defect Detection Experiment

In the defect-detection experiment, a beacon defect was detected, assuming a malfunction such as battery exhaustion, defect or movement of a beacon. The verified defect situation is shown in Fig. 7. In defect 1, one of three beacons in room A is unusable due to battery outage or malfunction. In defect 2, the beacons of room B and room C were arranged mistakenly, or moved. In defect 3, it is assumed that the beacon of room E has been moved to room D. In fact, in simple situations with
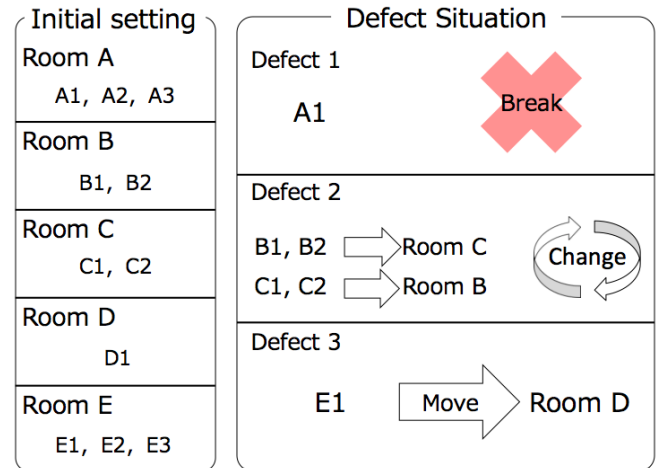
Figure 7: Assumed defect situation

Table 4: Defects that expected to be detected

Room name	Should not be observable	Observable but are not
RoomA	None	A1
RoomB	C1, C2	B1, B2
RoomC	B1, B2	C1, C2
RoomD	E1	None
RoomE	None	E1

only one beacon defect, our method can detect the defect easily. Therefore, we set these more complex situations for the experiment.

Figure 4 represents the details of defect situations. As Defect 1, Beacon A1 is broken, so that A1 cannot be observed in Room A. Therefore, the defect situation named "Observable but are not" should be detected in Room A. Also, there are no beacons to be moved to Room A, so that the defect situation named "Should not be observed" should not be detected in Room A. We set Defect 2 in Room B and C. The defect suppose misplacement by the system operator. Beacon B1 and B2, they should be placed in Room B, are misplaced in Room C. Also, Beacon C1 and C2, they should be placed in Room C, are misplaced in Room B. Therefore, both of the defect situations named "Observable but are not" and "Should not be observed" should be detected in Room B and C. Defect 3 is mischief situation. One of the beacon named E1 in Room E is moved to Room D by someone. Therefore, "Observable but are not" should be detected in Room E1, also "Should not be observed" should be detected in Room D. The result of detection is presented in Fig.6

Table 5 shows the detailed result of room estimation and defect detection. At first, the method estimates existing room. If observed room and estimated room are same, room estimation result is correct. Then, each defect is checked on the condition of the user observed in estimated room.

In defect 1, existing room is estimated as room A, and the estimation is correct. On the condition that the user observed

Table 5: Detailed result of defect detection

	Observed room	Room estimation result	Estimated room	Defect detection result	Estimated number of defects	
					Should not be observable	Observable but are not
Defect1	RoomA	Correct	RoomA	Correct	None	A1:10
				Wrong	None	None
Defect2	RoomB	Correct	RoomB	Correct	C1:10, C2:10	B1:10, B2:10
				Wrong	None	None
	RoomC	Wrong	RoomB	Correct	None	None
				Wrong	D1:7. E1:5	None
		Correct	RoomC	Correct	B1:4, B2:4	C1:4, C2:4
				Wrong	E1:1	None
		Wrong	RoomD	Correct	None	None
				Wrong	B1:6, B2:6, E1:4	D1:3
Defect3	RoomD	Wrong	RoomB	Correct	None	None
				Wrong	D1:10, E1:10	None
		Correct	RoomD	Correct	E1:10	None
				Wrong	B1:10, B2:10	None
	RoomE	Correct	RoomE	Correct	None	E1:10
				Wrong	None	None

Table 6: Accuracy of defect detection

	Should not be observable	Observable but are not
Total number of defect detections	107	51
Number of correct answers for defect detection	38	48
Incorrect number of defects detected	69	3
Correct answer rate	35%	94%

BLE/Wi-Fi signals in room A, BLE A1 was estimated 10 times as "Observable but are not". The defect detection is correct, so that "A1:10" is appeared in a cell of "Defect detection result - Correct" and "Observable but are not". Also, the defect "Should not be observable" should not be observed in room A, so that "None" is set in a cell of "Defect detection result - Wrong" and "Should not be observed". There are no estimation error in terms of defect 1. Therefore, "None" is set both of the cells of "Defect detection result - Wrong. "

In defect 2, room estimation was succeeded when the user exists in room B. On the condition that the user observed BLE/Wi-Fi signals in room B, BLE C1, C2 were estimated 10 times as "Should not be observed". Also, BLE B1, B2 were estimated 10 times as "Observable but are not". The defect detections are all correct, so that "C1:10, C2:10" appears in "Defect detection result - Correct" and "Should not be observable" and "B1:10, B2:10" are appears in "Defect detection result - Correct" and "Should not be observable". The number after colon means the number of defect detection times. On the other hand, in room C, room estimations contain errors as room B and room D, so that they are shown as "Wrong". If room estimation failed, the method tends to derive wrong defects. For example, when the room is wrongly estimated as room B, wrong defects of "D1:7. E1:5" appears in "Defect detection result - Wrong" and "Should not be observable". When the room is wrongly estimated as room D, wrong defects of "B1:6, B2:6, E1:4" appears in "Defect detection result - Wrong" and "Should not be observable". Also, wrong defects of "D1:3" appears in "Defect detection result - Wrong" and "Observable but are not". Even if the room estimation is correct, defect detection may contain errors. When the room is correctly estimated as room C, wrong defects of "E1:1" appears in "Defect detection result - Wrong" and "Should not be observable".

In defect 3, as same as defect 2, there are several defect detection failures even the room estimation is correct. The corresponding cell is, "Defect 3 - Room D - Correct - Room D - Wrong" and "Should not be observable", and the concrete defect detections are "B1:10, B2:10".

From Table 6, the number of defect detections is larger than the number of observations. In this research, we estimate rooms using BLE and Wi-Fi and detect defects of BLE. Therefore, the result will come up two estimating of the rooms for BLE and Wi-Fi. If the room estimation results using BLE and Wi-Fi are different, defects are detected for each estimated room. When the estimation of BLE is room A and the room estimation in Wi-Fi is room B, the result of defect detection in room A and defect detection in room B are obtained. Also, even if it is in the same room, there are cases where multiple defects such as "BLE A1 can not be observed" and "BLE A2 can not be observed". In the situation, the number of defect is counted for each defect. Therefore, the total number of defect detection will be larger than 50 observations. For example, BLE C1 and BLE C2, which do not exist in room B, were observed. The total number of defect detections is represented by the sum of correct and incorrect detections of "Should not be observable" and "Observable but are not" in Table 5, respectively. The number of correct answers for de-

fect detection is expressed by the sum of "Correct" each defect detection. The incorrect number of defects detected is expressed by the sum of "Wrong" each defect detection. The correct answer rate is represented by "total number of defects estimated / correct defect detections".

The first "Observable but are not" targets are rooms A, B, C and E from Table 6. The number of observations and the number of defects detected are not much different. In addition, the number of correct answers for defect detection is large, and the correct answer rate is 94%. For defect detection, rooms A, B, D and E are accurately detected. However, room B has detected a different BLE than expected. The next deficiency is "Should not be observed". Detectable estimation results are for rooms B, C, and D. The number of estimated defects is almost twice the number of observations. About one third of the correct answers are correct, and the correct answer rate is 35%.

As a consideration of defect detection, as shown in Table 5, in rooms A and E, the BLE of the other room cannot be seen. Therefore, "Should not be observable" and "Observable but are not" defects are detected correctly. It is thought that this is because the rooms are far away from each other, so their BLEs do not interfere with each other. Room B is separate from other rooms. Therefore, it is considered that it is not influenced by other beacons, and defects can be accurately detected. Rooms C and D are next to each other. Therefore, they are considered to be more affected by BLE compared to other rooms. As a result, as shown in Table 5, unexpected BLE is detected, and erroneous detection becomes a problem. From these results, it can be considered that it is possible to detect malfunction accurately when the room is separated and not affected by other beacons. However, if the room to be observed is close to another, the estimates of the room by BLE and Wi-Fi may be different. Therefore, it is considered that the number of detected defects increases and the number of correct answers for defects decreases. In this hypothesized defect experiment, it was executed assuming that all BLEs located in rooms B and C were replaced. Therefore, it is considered that a significant estimation error occurred between BLE and Wi-Fi.

5 CONCLUSION

In this paper, we proposed a BLE beacon defect detection method. The method is based on WiFi and BLE fingerprints for each room. We modeled the observed Wi-Fi and BLE data for each room. Basically, we compared the BLE model with the observed BLE list and estimated the room. We also compared Wi-Fi models and Wi-Fi lists at regular intervals.

A room-estimation experiment was conducted. We calculated the probability that room estimation would succeed. Also, we obtained the boundary value of the signal strength that does not affect beacon-defect estimation. We experimented with three boundary values: -50 dBm, -75 dBm, and -90 dBm. The best result was -75 dBm. Therefore, Wi-Fi signal that is under -75 dBm is removed for our method.

We conducted a beacon defect detection experiment, and it was possible to detect a beacon in which a malfunction had occurred. However, it was difficult to estimate a defect in a room with a neighboring room or a room with a small space. The reason for this is that beacons are confused because they are more vulnerable to nearby BLE radio waves. Isolated rooms could be detected with 100% accuracy. However, adjacent rooms could only be detected with 35% accuracy.

In this experiment, we observed data only in rooms. We did not observe BLE/Wi-Fi information in hallways. Therefore, there is a possibility that room estimation could be done even from a hallway. If you are in a room, you may mistake some room estimation if tracking for several tens of seconds. However, if the number of times estimated in the same room is large, you can presume that you are in the room.Also, in the case of a hallway, room estimation is considered to change one after another. Therefore, it can be presumed that you are walking in the hallway.

As future work, we should modify the BLE/Wi-Fi room model and improve room estimation accuracy. One idea is to introduce a Gaussian distribution model to express possible signal strength. By modeling with Gaussian distribution, we can understand the range of the radio-wave intensity seen in a specific room and consider that the room can be accurately estimated even with an adjacent room. If the room can be estimated accurately, it can be expected that the accuracy of estimation of beacon defects should be improved.

At the time of operation, it is possible to automatically update the room model by using the uploaded BLE/Wi-Fi observation data. If we keep the model we created first, we may not be able to estimate rooms, such as when a beacon is changed out or there are many people or things in the rooms. Therefore, we should update the model in operation. We believe that data of various situations can be observed and changed according to the situation and changes in the environment.

REFERENCES

[1] A. K. Arzad, K. B. Suleep, S. Bongjhin. "Hybrid location tracking in BLE beacon systems with in-network coordination". *2016 13th IEEE Annual Consumer Communications & Networking Conference (CCNC), pp. 814-815*, (2016).

[2] S. Noguchi, M. Niibori, Z. Erjing. "Student Attendance Management System with Bluetooth Low Energy Beacon and Android Devices". *2015 18th International Conference on Network-Based Information Systems, pp. 710-713*, (2015).

[3] R. Lodha, S. Gupta, H. Jain, H. Narula. "Bluetooth Smart Based Attendance Management System". *International Conference on Advanced Computing Technologies and Applications (ICACTA), Vol. 45, pp. 524-527*, (2015).

[4] T. Mori, S. Kajioka, T. Uchiya, I. Takumi, H. Matsuo. "Experiments of position estimation by BLE beacons on actual situations". *2015 IEEE 4th Global Conference on Consumer Electronics (GCCE), pp. 683-684*, (2015).

[5] F. Ramsey, H. Robert. "Location Fingerprinting With Bluetooth Low Energy Beacons". *IEEE Journal on Selected Areas in Communications, Vol. 33, Issue: 11, pp. 2418-2428*, (2015).

[6] S. S. Chawathe. "Beacon Placement for Indoor Localization using Bluetooth". *2008 11th International IEEE Conference on Intelligent Transportation Systems, pp. 980-985*, (2008).

[7] N. Allurwar, B. Nawale, S. Patel. "Beacon for Proximity Target Marketing". *International Journal Of Engineering And Computer Science, ISSN: 2319-7242 Vol. 5, pp. 16359-16364*, (2016).

[8] D. Asahi, Y. Yokohata, T. Inoue, H. Maeoomichi, A. Tsutsui. "Performance evaluation of user participation type BLE beacon operation monitoring in wide area electronic stamp rally experiment". *IEICE technical report, Vol. 115, No. 466, pp. 1-5*, (2016) (in Japanese).

[9] A. Yamaguchi, M. Hashimoto, K. Urata, Y. Tanigawa, T. Nagaie, T. Maki, T. Wakahara, A. Kodate, T. Kobayashi, N. Sonehara. "Beacon-based tourist information system to identify visiting trends of tourists". *The 2017 International Conference on Artificial Life and Robotics (ICAROB 2017), Vol. 4, pp. 209-212*, (2017).

[10] P. Dhruv, J. Ravi, L. C. Emil. "Indoor location estimation using multiple wireless technologies". *14th IEEE Proceedings on Personal, Indoor and Mobile Radio Communications, PIMRC 2003, Vol. 3, pp. 2208-2212*, (2003).

[11] S. Kajioka, T. Mori, T. Uchiya. "Experiment of indoor position presumption based on RSSI of Bluetooth LE beacon". *2014 IEEE 3rd Global Conference on Consumer Electronics (GCCE), pp. 337-339*, (2014).

[12] L. Peng, L. Qingbin, F. Qixiang, G. Xiangyou, H. Senying. "A Real-Time Location-Based Services System Using WiFi Fingerprinting Algorithm for Safety Risk Assessment of Workers in Tunnels". *Mathematical Problems in Engineering 2014. Vol. 2014, Article ID 371456, pp. 1-10*, (2014).

[13] R. Valentin, M. K. Mahesh. "Indoor Smartphone Localization via Activity Aware Pedestrian Dead Reckoning with Selective Crowdsourced WiFi Fingerprinting". *4th International Conference on Indoor Positioning and Indoor Navigation(IPIN 2013), pp. 1-10*, (2013).

[14] F. Arsham, L. Jiwei, K. M. Mahesh, J. G. Francisco. "A Microscopic Look at WiFi Fingerprinting for Indoor Mobile Phone Localization in Diverse Environments". *2013 International Conference on Indoor Positioning and Indoor Navigation, pp. 1-10*, (2013).

[15] H. M. Nizam, L. Sukhan. "Indoor Human Localization with Orientation using WiFi Fingerprinting". *Proceedings of the 8th International Conference on Ubiquitous Information Management and Communication, Article No. 109, pp. 1-6*, (2014).

Shota Ikeda is a graduate student at Aichi Institute of Technology. His current research focuses on estimating rooms using BLE beacons and detecting their defects. He is also interested in the Internet of Things and in creating a more convenient and less cumbersome society using BLE beacons.
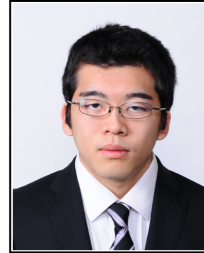
Fumitaka Naruse is an undergraduate student at Aichi Institute of Technology. His current research focuses on estimation of people in rooms using BLE beacons. His team developed an application linked to the web for acquiring real-time occupancy information and past occupancy history.

Katsuhiko Kaji received his Ph.D. in information science from Nagoya University in 2007. He became a RA at NTT Communication Science Laboratories in 2007 and an assistant professor in Nagoya University in 2010. Currently, he is associate professor of Faculty of Information Science, Aichi Institute of Technology from 2015. His research interests include indoor positioning and remote interaction. He is a member of IPSJ and JSSST.

Link-speed Aware Scheduling for Slotted-CSMA Based Wireless Mesh Networks

Yasuhiro Mori[†*] and Takuya Yoshihiro[‡**]

[†]Graduate School of Systems Engineering, Wakayama University, Japan
[‡]Faculty of Systems Engineering, Wakayama University, Japan
* s181056@sys.wakayama-u.ac.jp
** tac@sys.wakayama-u.ac.jp

Abstract - We focus on Slotted-CSMA based architecture of wireless mesh networks (WMNs) and propose a scheduling algorithm to eliminate hidden terminal effects even with high-speed IEEE802.11 links. To take high-speed links and its physical properties into account, we introduces so called the double-disk interference model in computing the scheduling algorithm that eliminates hidden-terminal effects that severely degrades the network performance. Also, toward the automated computation of schedules, we propose to measure the interference range of the double-disk model by incorporating beacons in IEEE 802.11. Through evaluation, we confirmed that the proposed scheduling algorithm works well in WMNs with high-speed links.

Keywords: Wireless Mesh Networks

1 INTRODUCTION

Wireless Mesh Networks (WMNs) has been deeply studied in the literature as a high-speed wireless network infrastructure to cover a large geometric area with less economical cost [1]. Aiming at wide applications utilized by general users, commodity IEEE 802.11 devices are often used in WMNs. Taking advantages of CSMA MAC, we can share precious frequency resources with many devices, which enable us to build WMNs on the shared bands such as 2.4 and 5GHz. We currently have a standard IEEE.802.11s that realizes to form a mesh network over Wi-Fi APs.

However, unfortunately, WMNs have not been succeeded so far due to heavy interference between wireless nodes. Although IEEE802.11 utilizes CSMA to avoid collisions [2], the simple carrier-sensing-based mechanism suffers from so called the hidden-terminal effects, which heavily degrades the communication performance. The well-known RTS/CTS handshake is typically used to cope with this problem [3] as is included in IEEE802.11 standard. However, the effect of RTS/CTS is known to be limited due to several reasons such as probabilistic collisions in RTS/CTS handshake, excessive suppression of transmissions known as the exposed terminal problem [4], and the inconsistency effects caused by difference between transmission range and interference range [5]. Even recently, IEEE802.11-based wireless mesh networks suffers from heavy interference among nodes [6].

To minimize the effect of interference, several studies propose *routing metrics* that reflects on the quality of wireless links that dynamically transits with time [7]-[9]. By computing the shortest paths with respect of routing metrics, we can choose the best paths with small interference. For example, Couto et al., proposed ETX that represents the expected transmission count of data frames under IEEE802.11 [7]. Draves et al., proposed ETT that represents the expected transmission time to transmit frames [8]. However, the effect of those routing-metric-based optimization is marginal since considerable amount of interference remains and degrades significantly the performance.

Many schemes using multiple frequency channels have been proposed to improve communication speed in wireless mesh network. References [8] [10] proposed routing metrics to minimize interference in WMNs in which each node has multiple network interface cards (NICs). Marina et al. proposed a greedy algorithm that statically assigns frequency channels to NICs [11] in order to minimize the interference in WMNs. Mo et al. compared and evaluated multi-channel MAC protocols where a single network interface dynamically switches communication channels among multiple channels [12]. However, these multi-channel schemes do not substantially improve the communication performance due to difficulty in timing synchronization between senders and receivers, and also due to the small number of available orthogonal channels under Wi-Fi, i.e., 3 channels.

On the other hand, several hybrid MAC protocols that take advantages of both CSMA and TDMA have been proposed mainly for wireless sensor networks. There are many of this kind such as IEEE 802.15.4 [13] standard, and the typical mechanism of them is to provide time slots in which CSMA and TDMA are dynamically selected to reduce frame collision [15] [16]. However, since they have been proposed for wireless sensor networks in which requirements for communication frequency are essentially different from WMNs, they cannot achieve the sufficient communication speeds required for WMNs.

To realize high-speed WMNs, Ding et al., proposed a scheme in [17] that combines the ADCA (Adaptive Dynamic Channel Allocation Protocol) and ICAR (Interference and Congestion Aware Routing protocol), where ADCA is an extension of MMAC [18] that distributedly negotiates channels for the multiple interfaces equipped on each node to reduce hidden terminal effects, and ICAR adaptively selects paths using dynamic metrics. However, although [17] is designed for the network with a gateway where the effect of interference is relatively small because all traffic goes through the gateway, ADCA cannot eliminate hidden terminal effects and so it reduces the interference using dynamic metrics.

CATBS(CSMA-Aware Time-Boundable Scheduling)[19] has been proposed as a method for solving the above problem and eliminate hidden-terminal effects in WMNs. CATBS is based on slotted CSMA, i.e., CSMA works within time-divided slots, and avoid collisions due to hidden-terminals by applying a schedule that assigns a slot for each link. Different from the previous studies, CATBS theoretically eliminates collisions due to hidden terminals by allowing detour paths in its joint routing and scheduling algorithm. Also, by introducing RTS/CTS in the slot boundaries, it is robust to the time drift on synchronizing time among nodes. As a result, CATBS achieves high-speed communications with low frame loss over WMNs.

However, one of the problems of CATBS comes from the interference model used in the scheduling scheme. The original scheduling scheme assumes a simple interference model called the single disk model in which the communication and the interference distances are the same. This is not a realistic property especially if CATBS works with high-speed communication links. In other words, the performance of CATBS will be significantly degraded with high-speed PHY protocols since the scheduling scheme does not match the physical property of communications.

The SINR model is widely known as a radio interference model close to reality [20]. The SINR (Signal to Interference and Noise Ratio) model regards the transmission signals as being received if the ratio of signal and noise (plus interference) is larger than a certain threshold. Note that, although SINR model is regarded as one of the standard models close to reality, if we design the scheduling problem based on SINR model, we need to consider all combinations of transmitting nodes to compute SINR so as to judge whether the transmission is succeeded or not, resulting in exponential computational time. Therefore, in the proposed method, we use the double disk model as a feasible interference model while being more realistic than the single disk model.

In this paper, we consider to use high-speed PHY in CATBS-based WMNs to raise the communication capacity of the networks. For this purpose, we first propose to introduce double-disk interference model in the scheduling scheme of CATBS. Note that double-disk interference model consists of two distances, i.e., the communication distance and the interference distance, and the latter is not easy to determine in the real environment. Thus, we next propose to determine the interference distance based on observation of IEEE802.11 beacons, which is transmitted with low-speed PHY protocol.

The reminder of this paper is organized as follows. In Sec. 2, we present CATBS, the baseline scheme of slotted-CSMA based WMNs. In Sec. 3, we extend CATBS by introducing double-disk interference model. In Sec. 4, we evaluate the proposed method. In Sec. 5 we introduce related work on joint routing and scheduling methods, and finally we conclude the work in Sec. 6.

2 CATBS: A SLOTTED-CSMA-BASED ARCHITECTURE OF WMNS

2.1 Overview

CATBS is a communication method for WMN that avoids hidden terminal problem, which is achieved with a combination of slotted CSMA and a scheduling method. In addition, the slotted CSMA used in CATBS is a little modified from the original CSMA. First, a single frequency channel is time-divided to create several virtually independent channels. Then, CSMA runs within each virtual channel. In the scheduling method, a virtual channel is allocated to each link such that hidden terminal problem does not occur. Since collision between adjacent nodes can be avoided by the carrier-sensing function of CSMA, our scheduling method only take the hidden-terminal effects into account. We define the interference model that considers radio interference due to hidden terminal problem and formulate it as an optimization problem that minimizes the effect of hidden terminal problem. Since the formulated problem is proven to be NP-hard, we obtain the solutions efficiently by reducing to PMAX-SAT.

2.2 MAC Protocol

The MAC protocol used in CATBS is a slotted CSMA with a little modification. The slotted CSMA is a mechanism in which we divide a frequency channel with a fixed time interval and run CSMA within each slot. Different from the original slotted CSMA, we do not use TDMA in slots at all because TDMA requires strict time synchronization. By avoiding to use TDMA, CATBS works with relatively loose time synchronization system, which significantly relaxes the restriction for the communication system.

In the MAC protocol used in CATBS, first, a single frequency channel is divided in time and multiple virtual channels are generated. Each virtual channel is called a slot. Then, CSMA runs inside the created slot. In order to operate CSMA, it is necessary to take a relatively large time per slot compared with TDMA. Each slot is given a number $1, 2, \cdots, k$ for identifying them, and it is switched in turn as $1, 2, ..., k, 1, 2, ...$ and so on. An example is shown in the Fig. 1. In Fig. 1, a single frequency channel is time-divided into k slots. Since two links in the relationship of hidden terminal problem transmit frames in different slots, the hidden terminal problem does not occur. In addition, RTS / CTS is used to avoid frame collision at the boundary of slots due to time synchronization error. Namely, when transmitting a data frame, if the transmission time is judged to exceed the boundary of the current slot, RTS is transmitted. After CTS is returned, nodes that received RTS or CTS wait for NAV period without transmitting data frames even if when the allocated slot comes. When the NAV period ends, the nodes start transmitting data frames.

2.3 Definitions

In order to formulate the scheduling problem, we begin with definitions. The network is represented by the directed graph $G = (V, E, C)$, where V is the node set, E is the link set, and C is the channel set. We define $e = (u, v, c)$ as
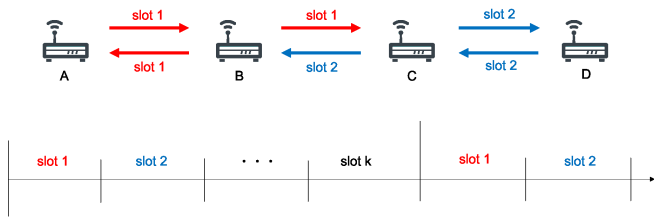
Figure 1: Virtual multi-channelization by time division
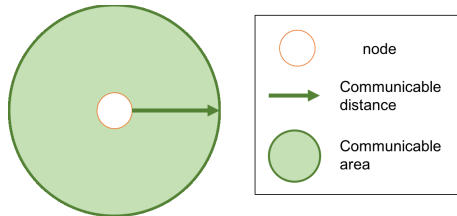
Figure 2: Communicable distance

the link to communicate using channel c from node $u \in V$ to $v \in V$. If there is a pair of links $e_1 = (u_1, v_1, c_1)$ and $e_2 = (u_2, v_2, c_2)$ in the hidden terminal relationship, it is called as an interference link pair. We denote the shortest path length from node u to v on graph G by $D^G_{(u,v)}$. Let S_G be the set of interference link pairs in G, which is called as the collision degree of graph G. The scheduling problem of CATBS aims at minimizing the number of collision link pairs $|S_G|$ by removing links in G and output the graph G' that is free from hidden terminal problem.

2.4　Single-disk Interference Model

CATBS uses a single disk model as an interference model to simplify the situation where radio interference occurs. In the single disk model, when a node communicates with some other nodes, the distance with which the communication succeeds is called the communicable distance r, and the area inside the circle of radius r is called the communicable area. In the single disk interference model, we assume that there is no radio interference outside the communicable area.

2.5　Defining Collision Link Pairs Based on Single Disk Model

Collisions under single disk model are modeled as two types: collisions invoked by data frames, and those invoked by Ack frames. We show an example of those two types of collisions in Fig. 3. In Fig. 3(a), a data frame from u_1 to v_1 collides with a frame from u_2 to v_2. In Fig. 3(b), an Ack frame sent from v_1 collides with a frame from u_2 to v_2. Those two types of collisions are formally defined as follows.

Type 1: collision with data frames occur if all the following conditions are met.

1. $c_1 = c_2$
2. $(u_1, u_2, c_1) \notin E$
3. $(u_1, v_2, c_1) \in E$

(a) Data frame interferes　　(b) Ack frame interferes
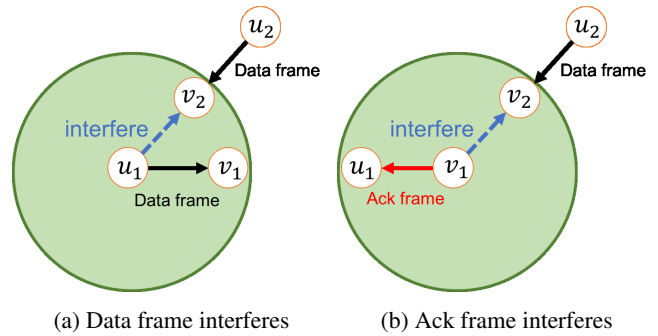
Figure 3: conditions of interference link pairs

Type 2: collision with Ack frames occur if all the following conditions are met.

1. $c_1 = c_2$
2. $(u_1, u_2, c_1 \notin E)$
3. $(v_1, v_2, c_1) \in E$

2.6　Formulation of Scheduling Problem

In the scheduling problem formulation of CATBS, we first consider the graph G that consists of every possible links $e = (u, v, c)$ where $u, v \in V$ and $c \in C$, i.e., we include links with every combinations of u, v, c. Then, we choose a subset of links in G and output the schedule $G' = (V, E', C)$ where $E' \subseteq E$. Note that, from the restriction of the default router architecture that each node has only one transmission queue, the number of slots assigned to a node is limited to one. Namely, the incoming and the outgoing links of the same node must belong to the same slot. Also note that the pair of links in the relationship of collision has already defined. Our goal is to minimize the *interference level*, which is defined as the number of collision link pairs in G'.

If the number of slots in the schedule increase, CATBS would face in severe end-to-end delay due to the time to wait active slot at each node. To prevent the delay in scheduling, CATBS allow to use paths that are not the shortest-paths between the source and destination node pairs. Specifically, in the scheduling, CATBS chooses a set of links for G' such that, for each pair of source and destination (s, d), the length of the shortest path in G' is equal to or less than that in $G + k$, where k is the predefined stretch factor. More formally, if we let $\delta^G_{s,d}$ be the shortest-path length from s to d in G, $\delta^{G'}_{s,d} \leq \delta^G_{s,d} + k$. Namely, by allowing k-hop longer paths than the shortest path, CATBS reduces the number of slots required to achieve zero-collision. As above, the formal description of the scheduling problem in CATBS is given as follows.

The Scheduling Problem in CATBS

Input: A graph $G = (V, E, C)$, A set of collision link pairs S_G.

Output: A schedule $G' = (V, E', C)$ where $E' \subseteq E$

Subject to: $\delta^{G'}_{s,d} \leq \delta^G_{s,d} + k$, and every node does not have more than 2 assigned slots.

Minimize: Interference level $|S_{G'}|$

2.7　Algorithm to Solve the Problem

In the literature the scheduling problem was proven to be NP hard. Therefore, it takes a huge amount of time to find the optimal solution. In CATBS, in order to find an approximate solution efficiently, we reduce the scheduling problem to PMAX-SAT. PMAX-SAT is a traditional NP-hard optimization problem, and recently, there held a contest of good solvers for large-scale PMAX-SAT problems, for which several excellent solvers have been developed so far. CATBS intends to use one of those excellent solvers of PMAX-SAT.

In PMAX-SAT, we let $x_1, x_2, ..., x_n$ be logical variables that take values true (1) or false (0). Let $\overline{x_1}$ be the inverted value of logical variable x_1. A logical expression such as $(x_1 \vee x_2)$ obtained by connecting several logical variables with OR operators $(\vee)$ is called a clause. We call logical expressions in which we connect clauses with AND operator $(\wedge)$ as a canonical normal form (CNF) formulas, e.g., $(x_1 \vee x_2) \wedge (\overline{x_1} \vee x_3)$. For each of the logical variables $x_1, x_2, ..., x_n$ in the given CNF formula we assign a logical value true(1) or false(0). The SAT(SATisfiability Problem) problem is defined as a task to output whether there is a set of true/false assignment that satisfy the given CNF formula. The problem to maximize the number of satisfied clauses is called MAX-SAT (MAXimum SATisfiability problem). As a further extension of MAX-SAT, we define Partial MAX-SAT (PMAX-SAT). For a given CNF formula $f(x_1, x_2, ..., x_n) = g_h(x_1, x_2, ..., x_n) \vee g_s(x_1, x_2, ..., x_n)$ where $g_h(\cdot)$ and $g_s(\cdot)$ are also CNF formula called hard and soft clauses, respectively, PMAX-SAT maximize the number of satisfied clauses in soft clauses g_s under the constraint that all the hard clauses g_h are satisfied. The formal description of PMAX-SAT is as follows.

　　PMAX-SAT

Input: CNF formula $f = g_h \vee g_s$.

Output: 0/1-Assignment of logical variables.

Maximize: The number of satisfied soft clauses.

Subject to: All hard clauses are satisfied.

We make a reduction from the scheduling problem of CATBS to PMAX-SAT. The constraints of CATBS such as the increase of path length are expressed by the hard clauses, and optimization criterion, i.e., the interference level, is expressed by the soft clauses. Specifically, for the input of the scheduling problem $G = (V, E, C)$, we define logical variables $l_{u,v,c}$ for all links included in E, where $l_{u,v,c}$ takes true if the corresponding link exists in G' and false otherwise. Although we omit the detail due to paper limitation, the hard clauses g_h are created such that they all are satisfied only if all the constraints in the scheduling problem are satisfied. See reference [11] for detail. The soft clauses g_s consists of a set of clauses $(\overline{l_1} \vee \overline{l_2})$, each of which corresponds to each collision link pair (l_1, l_2) in G. This clause does not satisfy only if both links are included in G' and invoke collision. As a result, once the PMAX-SAT is solved, the set of binary variables $l_{u,v,c}$ determines the schedule G', with which the interference level $|S_{G'}|$ is minimized. When this formula is a hard clause and

the hard clause is true, the graph G' satisfies the constraints of the optimization problem. Next, in the soft clause, the logical expression $(\overline{l_1} \vee \overline{l_2})$ for all the link pairs included in the set of link pairs S'_G in the hidden terminal problem relationship Take it with an AND operator. $(\overline{l_l} \vee \overline{l_j})$ takes false if both link pairs in hidden terminal problem relationships are not restricted on graph G'. That is, the number of logical expressions that take false matches the collision degree on graph G'. Then, by allocating logical variables that takes as many true as possible in soft clauses, graph G' eith lowest collision degree is output.

2.8　The Problem with CATBS-based WMNs

CATBS uses the single disk model to simplify the situation of hidden terminal problem. However, wireless communication gets more vulnerable against noise when the communication speed gets higher. Specifically, with high-speed links, the communicable distance goes shorter while the interference distance stays the same. As a result, when we assume high-speed links, schedules based on the single-disk model are no more possible to treat collisions appropriately. From this reason, we in this paper introduce the double-disk interference model to compute schedules more suitable for high-speed wireless communications.

3　THE PROPOSED METHOD

3.1　overview

We propose a new scheduling method to reduce radio interference in WMNs with high speed links. In our proposal, we use a double disk model as a more realistic interference model than the single disk model. In the double disk model, two distances, i.e., the communicable distance and the interference distance are defined such that two nodes can communicate with each other if they are located within the communicable distance, but a radio from a node located within the interference distance disturbs it. Our scheduling method is designed for distributed environment. First, we describe the method to identify the nodes within the range of the interference distance. We next give the algorithm to compute the collision link pairs from that information. After those steps, we can compute the schedule based on the double disk model.

3.2　Concept of proposed method

We intend to realize autonomously decentralized networks in which each node executes schedules and forwarding paths by means of running routing protocols. In the schedule calculation, each node requires the information of the network topology, so that a routing protocol such as OLSR is used to perform the distributed control. In order to realize the autonomous distributed scheduling using a routing protocol, each node needs to grasp the node located in the interference area under the double disk model. However, since the interference distance is larger than the communication distance especially with high-speed links, this information cannot be grasped by control messages of routing protocols. Also from the proactive routing protocol, each node cannot grasp the

distance information to identify the nodes in the interference distance because this kind of routing protocols only treats the topology of the network.

To grasp the nodes within the interference area, we use beacons that is periodically transmitted by every node with low communication speed. By observing all beacons received at every node, it grasps a set of nodes from which beacons can be received with high probability. Each node regards that the set of nodes are within the interference area. Since beacons are specified to transmit with minimum possible speed, the interference distance is supposed to be far larger than communicable distance.

In order to perform the distributed control using routing protocols, it is necessary that the calculation time of the schedule should be short and schedules should be computed even on a terminal with low capability. Simultaneously, we must design a joint routing and scheduling protocol in which schedules and routing tables are surely computed and the routing scheme works. In this paper, we simply introduce a feasible design of the joint routing and scheduling protocol that works in the distributed environment, and propose the method that can incorporate with the protocol.

3.3 Routing and Scheduling Protocol Framework

In order to execute the proposed scheduling method autonomously and distributedly, each node must collect the information required for scheduling. To compute schedules, we must collect two sorts of information, i.e., the network topology, and a set of collision link pairs. The network topology can be collected by using a proactive routing protocol such as OLSR. Therefore, we in this paper describe only how to collect collision link pairs.

In our joint routing and scheduling protocol, each node first computes its schedule (as we mentioned before, a schedule G' is a subgraph of the network topology G), and computes the shortest paths on G' to build its routing table. To compute a schedule, we must collect the network topology and the set of collision link pairs. To compute the latter, each node observes beacons and grasps a set of nodes within the interference area. On the other hand, the nodes within the communicable distance is known from the network topology. By sharing those two sorts of information with the surrounding nodes, each node can compute the collision link pairs. The set of collision link pairs computed at every node is shared over the network, and all nodes in the network obtains the set of collision link pairs as a result. Since every node know the topology and the collision link pairs of the whole network, a joint routing and scheduling protocol as described above is able to design. As the framework we apply the proposed scheduling algorithm, we assume this kind of network protocols.

3.4 Defining Collision Link Pairs Based on Double Disk Model

In the proposed method, we apply double disk model as the interference model to take the radio interference under high-speed links into account. The double disk model is defined
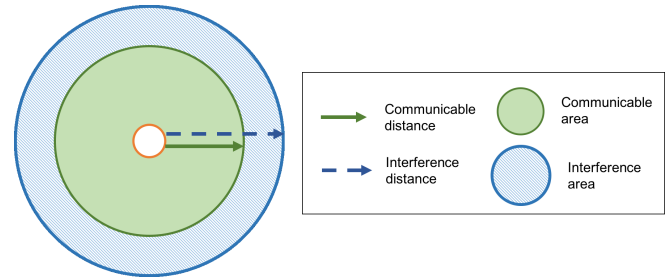
Figure 4: Interference distance

as two disks with different radius, which represents the communicable area and the interference area, respectively. In this interference model, the communicable distance (i.e., radius) means that two nodes are communicable with each other if other radio does not exist. Similarly, the interference distance means that the communication from a node s to d fails if d is within the interference distance from a node i on which transmission is ongoing. Generally, in high-speed links, the communicable distance is far smaller than the interference distance.

In order to formulate the scheduling problem, we make definitions of collision link pairs. For the network represented by a directed graph $G = (V, E, C)$, we assume two links as $e_1 = (u_1, v_1, c_1)$ and $e_2 = (u_2, v_2, c_2)$, and define the condition in which e_1 interferes e_2 due to the hidden terminal effect. Here, we denote the set of nodes located in the interference area of u_1 by N_{u_1}.

As in the case of CATBS, collisions are classified into two patterns: one is the case where data frames collide to other frames, and the case Ack frame collides. An example is shown in Fig. 5. In Fig. 5(a), the data frame from u_1 to v_1 collides to another frame from u_2 to v_2. In contrast, In the case of Fig. 5(b), the Ack frame from v_1 to u_1 collides to another frame from u_2 to v_2. The formal representation of those two type of collision cases are written as follows.

Type 1: collision with data frames occur if all the following conditions are met.

  1. $c_1 = c_2$
  2. $u_2 \notin N_{u_1}$
  3. $v_2 \in N_{u_1}$

Type 2: collision with Ack frames occur if all the following conditions are met.

  1. $c_1 = c_2$
  2. $u_2 \notin N_{u_1}$
  3. $v_2 \in N_{v_1}$

4 EVALUATION

4.1 Evaluation method

We evaluate the effectiveness of the proposed method in high speed communication environment through simulation

(a) Data frame interferes　　　(b) Ack frame interferes
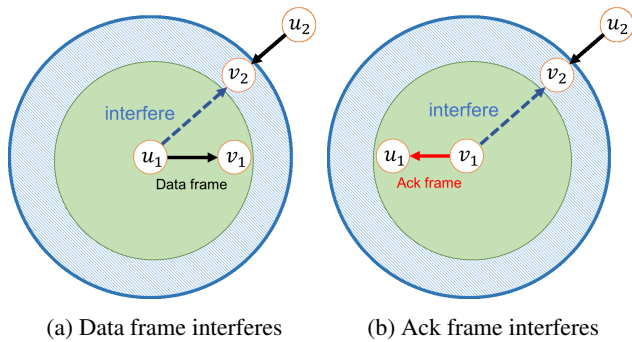
Figure 5: Conditions of interference link pairs

with the proposed scheduling method using network simulator Scenargie[21]. Since the proposed method uses the Double Disk Model, it is necessary to properly determine the communicable distance and the interference distance. To determine those values, we conducted a preliminary experiment by simulation.

The proposed method is designed to perform scheduling calculation using information that can be acquired in an autonomous distributed environment. As we mentioned previously, if data frames can be received from an adjacent node with high probability, we regard that the node is within the range of the communicable distance. On the other hand, if a beacon frame can be received from a node, we regard that the node is within the interference distance range. In this evaluation, we evaluate the communication performance by applying a pre-calculated schedule instead of calculating schedules in real time due to computational time for scheduling. In order to determine the appropriate communicable distance and the interference distance used in the schedule calculation in advance of performance evaluation, we carried out a preliminary simulation to determine those two distances.

With preliminary simulations, we first retrieve for each node a set of nodes within the communication and interference distance, respectively. Specifically, we run simulation with the scenarios planned in traffic simulation, find the set of nodes from which more than 80% of data frames are received, and identify the set as within communication distances. Similarly, we find the set of nodes from which more than 80% of beacon frames are received, and identify it as the nodes within interference distances. Those two sets of nodes are used in computing schedules, i.e, we create a PMAX-SAT formula from those sets and the topology, and compute a schedule by solving the PMAX-SAT problem. As PMAX-SAT solver, we used qmax-sat developed by Koshimura[22].

As a simulation scenario that is common in both the preliminary simulation and the traffic evaluation given in Sec. 4.3, we located 100 nodes in the 2300×2300 meter rectangular field, and generate 40 flows with randomly selected source and destination nodes. In the flows, packet size is 1500 Bytes and the transmission rate is 1 Mbps each. Each node communicates with others under IEEE802.11g standard with 48 Mbps speed and 20 dBm transmission power. According to the standard, beacon frames are transmitted with 1 Mbps speed. We generate flows from the beginning of the scenario, and measure the performance in the interval of stable state from

60 Sec to 600 Sec.

We first evaluate the performance of schedules obtained with our method, and next made a traffic evaluation to examine the communication performance. In the former evaluation, we investigate the number of slots necessary to achieve zero collision. In the proposed method, double-disk model is used as the interference model. Therefore, it is conceivable that the number of slots required for zero collision goes larger than CATBS. In the evaluation, it is clarified how much the number of slots is needed compared with CATBS.

In traffic simulation, we evaluate the communication performance of the proposed method in comparison with CATBS. We generate 40 flows with randomly-selected sources and destinations in various transmission rates. Same as the preliminary simulation, we measured the communication performance in the time interval from 60 Sec to 600 Sec to avoid capturing the unstable state of networks. We ran the simulation 10 times for each parameter values and use the average of it.

4.2　Scheduling performance

We examine the number of slots required to achieve zero-collision for each value of stretch factor k over the random topology. As shown in Fig. 6(a), CATBS could not compute zero-collision schedule with $k \leq 4$ even under as large as 9 slots. In contrast, Fig. 6(b) shows that the proposed method computes a zero-collision schedule even for the 5-slot case with $k \leq 4$. This is mainly because the carrier-sense distance in the proposed method, which is set to the same value as interference distance, is larger than CATBS. By introducing the double-disk model, not only the interference range but also the carrier-sense range increases. This improves the spacial efficiency, resulting in zero-collision schedule under smaller number of slots.

From above, we conclude that the proposed method reduces the required number of slots to obtain a zero-collision schedule. This means that the favorable effect of larger carrier sense distance is larger than the inconvenient effect of larger interference distance. For practical use, the proposed model is more favourable than CATBS in that zero-collision schedule is easier to obtain.

4.3　Communication performance

We compare the communication performance of the proposed method with CATBS using network simulator Scenargie [21]. We first compare the performance under several parameter values within the proposed method and CATBS, respectively, and finally compare those two with the best-performance parameters.

First, we show the results on CATBS in Fig. 7. Since CATBS could not achieve zero-collision, we examined the results of 4-5 slots with small k, and added the results of 3 slots for reference. From the results, the case of 4 slots with $k = 0$ leads the best performance. For each number of 4-5 slots, the case of $k = 0$ is better than $k = 1$, meaning that the penalty of longer paths is larger than the loss of collision with shorter paths in CATBS. Note that, with $k = 0$, although the 5-slot
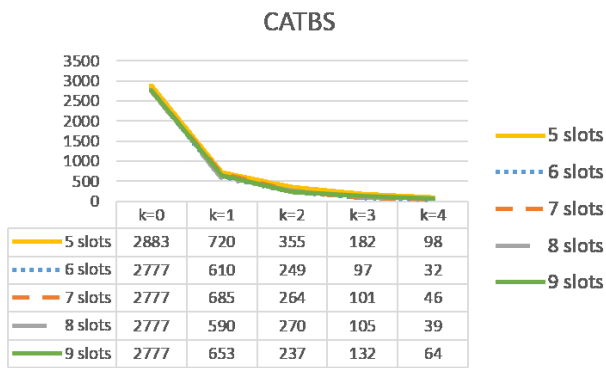
(a) Interference levels based on Single Disk Model (CATBS)
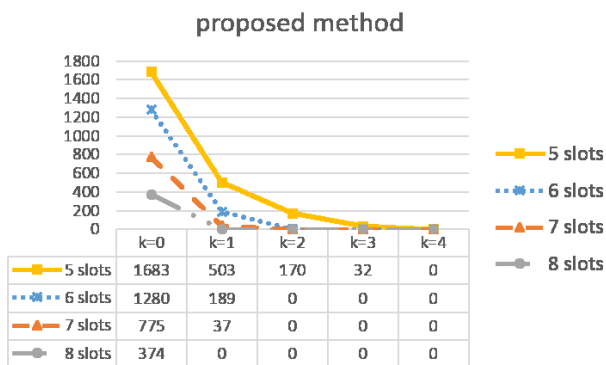
(b) Interference levels based on Double Disk Model (proposed method)

Figure 6: Scheduling

case exhibits almost the same thoughput performance as the 4-slot case, delay paerformance is degraded. This is because, in 5-slot cases, smaller capacity of links due to larger number of slot causes queuing delay. Anyway, the case of 4-slot with $k = 0$ was the best in CATBS.

Next, we compare the results on the proposed method in Fig. 8. From the results on the scheduling algorithm, we identified the cases of 6-8 slots with $k \leq 2$ as the suitable parameter values in practical use. Among the cases of 6-7 slots, the case with $k = 2$ has the best performance. This means that collision reduction achieved by longer paths effectively works in the proposed method, which is a different trend from CATBS. With 8 slots, the case of $k = 1$, the smallest k with zero-collision schedule, has the best performance, where the trend is the same trend as 6-7 slot cases. The best case is with 6 slots and $k = 2$, since smaller number of slots naturally improves both delay and capacity, and also since sufficiently large k achieved zero-collision.

We compared the performance of CATBS, CSMA and the proposed method. We use the case of 4 slots with $k = 0$ for CATBS, and two cases of 6 slots with $k = 2$ and 8 slots with $k = 1$ for the proposed method. See Fig. 9 for the results. The proposed methods marks higher performance than CATBS although the number of slots is larger than CATBS. This is mainly due to the effect of achieving zero-collision by offering longer paths. CSMA is lower than the proposed methods in both throughput and delivery ratio although delivery delay is always low. This is due to high frame loss ratio

caused by hidden terminals in CSMA. It is concluded that the proposed method improves the communication performance under high-speed links by introducing the double disk model.

Finally, we compared the performance in TCP communications. The simulation scenario is the same except that we generate 60 TCP flows with random source and destination nodes. The results are shown in Fig. 10(a)(b). Although the delivery ratio of the proposed method is higher than CATBS and achieves almost 100%, the throughput is lower. This is due to low link capacity of the proposed method, i.e., since the number of slots in the proposed method is 1.5 times larger than CATBS, link capacity per link is 1.5 times lower, and throughput is 1.5 times lower as well. This offers a weakness of the proposed method that requires a larger number of slots in expense of reducing packet loss.

5 RELATED WORK

we already have several joint channel assignment and routing schemes in the literature. Since channel assignment is essentially the same as slot allocation, they are closely related to CATBS. Alicherry et al. proposed a joint channel assignment and routing method that tries to optimize throughput in WMNs in multiple gateway scenarios by combining Linear Programming (LP) with their heuristic algorithms [24]. However, since they do not assume the property of CSMA, i.e., they assume that every adjacent link pair interferes with each other, the required number of channels grows too large so that they cannot achieve collision-free channel assiignment even with as many as 12 orthogonal channels. Mohsenian-Rad et al. proposed a joint channel assignment and routing method that considers path-length constraint in general WMNs by applying Mixed Integer and Linear Program (MILP) [23]. However, since they assume that RTS/CTS is always used and that it works perfectly under the single-disk interference model, their method has less efficiency due to exposed terminal problems, and further suffers from interference in high-speed environments due to the gap between the single-disk interference model and reality. By applying more precise collision model based on CSMA on top of double-disk model, the proposed method achieves more efficient collision-free schedule.

6 CONCLUSION

In this paper, we proposed a new scheduling method to reduce radio interference under high speed communication. By using the double disk model as an interference model, more precise treatment of radio interference is possible compared to the conventional single disk model. The proposed scheduling algorithm based on the double disk model, a large part of collisions that are involved in the schedule in CATBS are avoided.

As a result of the evaluation, we confirmed that, by using the proposed scheduling method, radio interference under high speed communication is reduced and communication performance is improved. From this fact, modeling using the double disk model is more suitable than using the single disk model under high-speed communication. In addition, the proposed method uses beacon reception status to determine the

(a) CATBS throughput   (b) CATBS Packet Delivery Rate   (c) CATBS Packet Delivery Delay
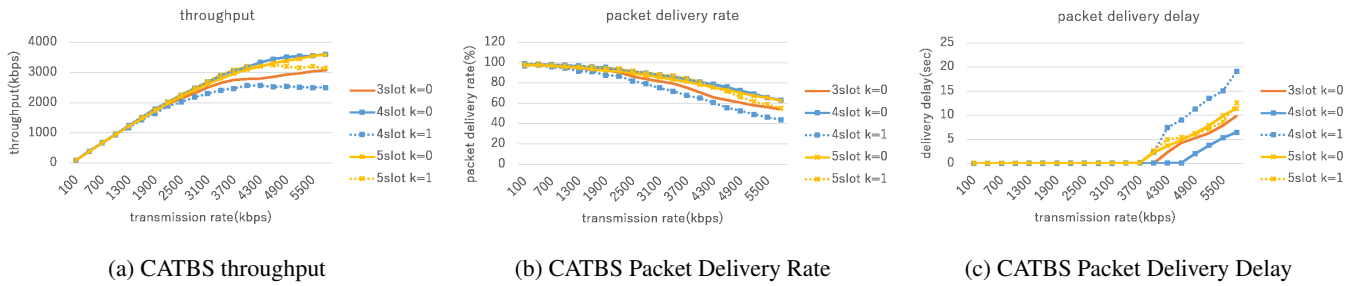
Figure 7: Comparing Performance of CATBS Under Parameter Variation

(a) propose method Throughput   (b) propose method Packet Delivery Rate   (c) propose method Packet Delivery Delay
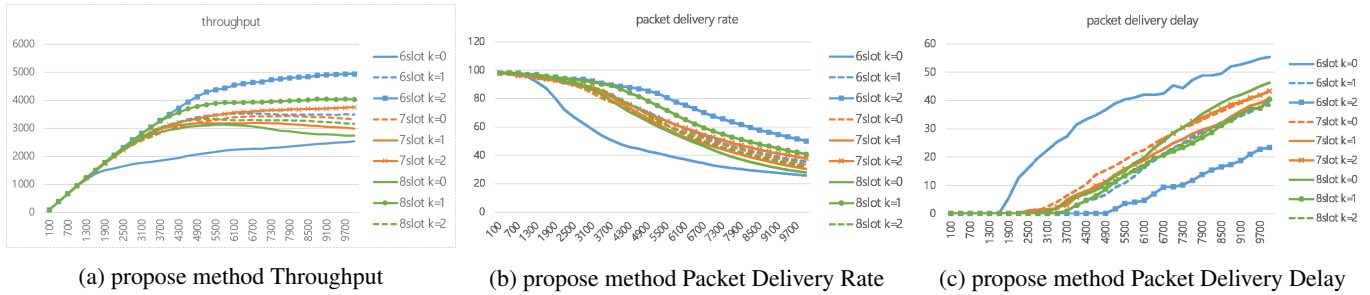
Figure 8: Comparing Performance of Proposed Method Under Parameter Variation

interference distance. Our evaluation in this paper shows that we can grasp the interference distance with this approach, and indicates the possibility that we could design autonomous distributed joint routing and scheduling scheme in the future.

One of the future tasks is to apply more realistic interference models in scheduling. The double disk model considers the interference range in addition to the single disk model. However, the most realistic interference model called SINR model judges whether frames are successfully received or not from SINR (Signal and Interference plus Noise Ratio). SINR-model-based scheduling would offer more accurate scheduling and would further improve the spacial efficiency of wireless communications.

In addition, we note that the beacon-based determination of double-disk-model distances proposed in this paper cannot determine the suitable distances for various communication speed. This paper showed that the proposed method determines the two distances of the double-disk model suitable for 48Mbps speed. However, the suitable distances are in fact different for each speed. How to determine them for each communication speed and modulation method is also left in the future.

ACKNOWLEDGMENT

REFERENCES

[1] I. Akyildiz and X. Wang, Wireless Mesh Networks, John Wiley & Sons, Ltd., Publication (2009).

[2] IEEE802.11 Wireless local Area Networks, http://www.ieee802.org/11/ (referred in Feb 2017).

[3] B. Bharghavan et al., "MACAW: A Media Access Protocol for Wireless LANs," In Proc. ACM SIGCOMM'94 (1994).

[4] J.L. Sobrinho, R. de Haan, J.M. Brázio, "Why RTS-CTS Is Not Your Ideal Wireless LAN Multiple Access Protocol," In Proc WCNS'05 (2005).

[5] K. Xu, M. Gerla, and S. Bae, "Effectiveness of RTS/CTS Handshake in IEEE 802.11 Based Ad Hoc Networks," Ad Hoc Networks, Vol.1 Issue.1, pp.107-123 (2003).

[6] R.K. Sheshadri and D. Koutsonikolas, "Comparison of Routing Metrics in 802.11n Wireless Mesh Networks," The 32nd IEEE International Conference on Computer Communications (INFOCOM'13) (2013).

[7] D. De. Couto, D. Aguayo, J. Bicket, and R. Morris "A High-Throughput Path Metric for Multi-Hop Wireless Sensor Networks," Proceedings of the 9th annual international conference on Mobile computing and networking (MOBICOM'03), pp.134-146 (2003).

[8] R. Draves, J. Padhye, and B. Zill, "Routing in Multi-Radio,Multi-Hop Wireless Mesh Networks, Proceedings of the 10th annual international conference on Mobile computing and networking (MOBICOM'04)," pp.114－128 (2004).

[9] V.C.M. Borges, M. Curado, and E.Monteiro, "The impact of interference-aware routing metrics on video streaming in Wireless Mesh Networks," Ad hoc networks, Elsevier (2011).

[10] H. Kanaoka and T. Yoshihiro, "Combining Local Channel Selection with Routing Metrics in Multi-channel Wireless Mesh Networks," IPSJ Journal of Information Processing (JIP), Vol.23, No.2 (2015).

[11] M.K. Marina, S.R. Das, A.P. Subramanian, "A topology control approach for utilizing multiple channels in

(a) Throughput

(b) Packet Delivery Rate

(c) Packet Delivery Delay
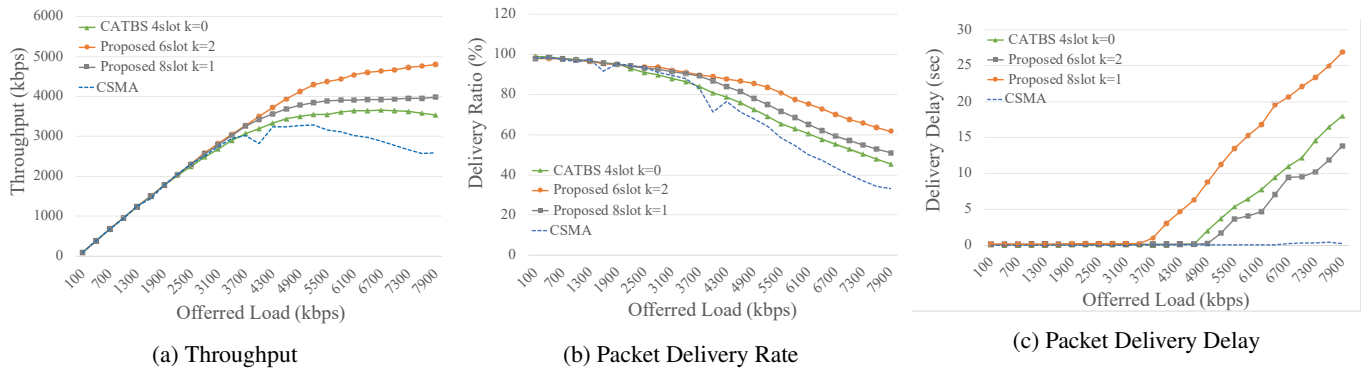
Figure 9: CBR Performance Comparison

(a) Packet Delivery Rate

(b) Throughput
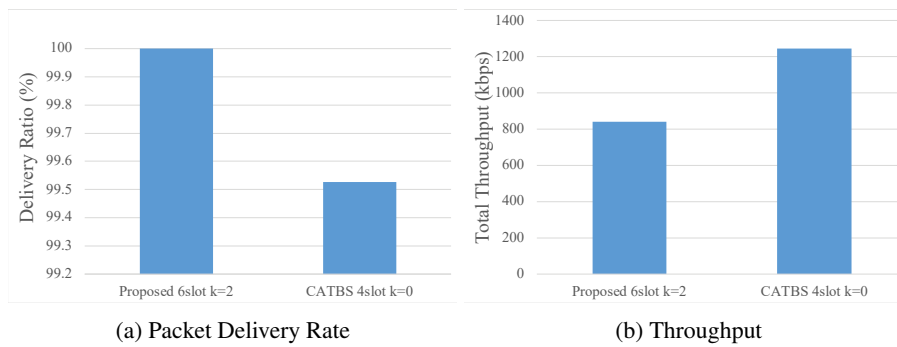
Figure 10: TCP Performance Comparison

multi-radio wireless mesh networks," Computer Networks, Vol.54, pp.241-256 (2010).

[12] J. Mo, H.S So, and J. Walrand, "Comparison of Multichannel MAC Protocols," IEEE Transactions on Mobile Computing, Vol.7 Issue.1 (2008).

[13] IEEE802.15.4b standard, Wireless Medium Access Control and Physical Layer Specification for Low Rate Wireless Personal Area Networks (2006).

[14] D. Yang, Y. Xu, and M. Gidlund, "Wireless Coexistence between IEEE 802.11- and IEEE 802.15.4-Based Networks: A Survey," International Journal of Distributed Sensor Networks (2011).

[15] W.L. Lee, A. Datta, R. Cardell-Oliver, "FlexiTP: A Flexible-Schedule-Based TDMA Protocol for Fault-Tolerant and Energy-Efficient Wireless Sensor Networks," IEEE Transactions on Parallel and Distributed Systems, Vol.19, Issue.6 (2008).

[16] I. Rhee, A. Warrier, M. Aia, J. Min, and M. L. Sichitiu, "Z-MAC: A hybrid MAC for wireless sensor networks," IEEE/ACM Trans. Netw., vol. 16, no. 3, pp. 511-524 (2008).

[17] Y. Ding, K. Pongaliur, and L. Xiao, "Channel Allocation and Routing in Hybrid Multichannel Multiradio Wireless Mesh Networks," IEEE Transactions on Mobile Computing, Vol.12, No.2 (2013).

[18] J. So and N. Vaidya, "Multi-channel Mac for Ad Hoc Networks: Handling Multi-channel Hidden Terminals Using a Single Transceiver," Proc. of ACM MobiHoc (2004).

[19] T. Yoshihiro and T. Nishimae, "Practical Fast Schedul-

ing and Routing over Slotted CSMA for Wireless Mesh-Networks," In Proc. of IEEE/ACM International Symposium on Quality of Service (IWQoS2016), 2016.

[20] P. Gupta and P. Kumar, "The capacity of wireless networks," IEEE Transactions on Information Theory, Vol. 46, No. 2, pp.388-404 (2000).

[21] Network Simulator Scenargie, Space Time Engineering, available from https://www.spacetime-eng.com/jp/ (referred in Jan 2017).

[22] M. Koshimura, T. Zhang, H. Fujita, R. Hasegawa, "QMaxSAT: A Partial Max-SAT Solver," Journal on Satisability, Boolean Modeling and Computation, Vol.8, pp.95-100 (2012)

[23] A.H. Mohsenian-Rad and V.W.S. Wong, "Joint Logical Topology Design, Interface Assignment, Channel Allocation, and Routing for Multi-Channel Wireless Mesh Networks," IEEE Transactions on Wireless Communications, Vol.6, No.12 (2007).

[24] . M. Alicherry, R. Bhatia, and E.L. Li, "Joint Channel Assignment and Routing for Thssroughput Optimization in Multi-radio Wireless Mesh Networks," IEEE Journal on Selected Areas in Communications, Vol. 24, No. 11 (2006).

Yasuhiro Mori received his B.E. degree from Wakayama University in 2017. He is currently a Master-course student in Wakayama University. He is interested in wireless networks and communications.

Takuya Yoshihiro received his B.E., M.I. and Ph.D degrees from Kyoto University in 1998, 2000 and 2003, respectively. He was an assistant professor in Wakayama University from 2003 to 2009. He has been an associate professor in Wakayama University from 2009. He is currently interested in the graph theory, distributed algorithms, computer networks, medial applications, and bioinformatics, and so on. He is a member of IEEE, IEICE, and Senior member of IPSJ.

Submission Guidance

About IJIS

International Journal of Informatics Society (ISSN 1883-4566) is published in one volume of three issues a year. One should be a member of Informatics Society for the submission of the article at least. A submission article is reviewed at least two reviewer. The online version of the journal is available at the following site: http://www.infsoc.org.

Aims and Scope of Informatics Society

The evolution of informatics heralds a new information society. It provides more convenience to our life. Informatics and technologies have been integrated by various fields. For example, mathematics, linguistics, logics, engineering, and new fields will join it. Especially, we are continuing to maintain an awareness of informatics and communication convergence. Informatics Society is the organization that tries to develop informatics and technologies with this convergence. International Journal of Informatics Society (IJIS) is the journal of Informatics Society.

Areas of interest include, but are not limited to:

Internet of Things (IoT)	Intelligent Transportation System
Smart Cities, Communities, and Spaces	Distributed Computing
Big Data, Artificial Intelligence, and Data Science	Multi-media communication
Network Systems and Protocols	Information systems
Computer Supported Cooperative Work and Groupware	Mobile computing
Security and Privacy in Information Systems	Ubiquitous computing

Instruction to Authors

For detailed instructions please refer to the Authors Corner on our Web site, http://www.infsoc.org/.

Submission of manuscripts: There is no limitation of page count as full papers, each of which will be subject to a full review process. An electronic, PDF-based submission of papers is mandatory. Download and use the LaTeX2e or Microsoft Word sample IJIS formats.

http://www.infsoc.org/IJIS-Format.pdf

LaTeX2e

LaTeX2e files (ZIP) http://www.infsoc.org/template_IJIS.zip

Microsoft Word^{TM}

Sample document   http://www.infsoc.org/sample_IJIS.doc

Please send the PDF file of your paper to secretariat@infsoc.org with the following information:

Title, Author: Name (Affiliation), Name (Affiliation), Corresponding Author. Address, Tel, Fax, E-mail:

Copyright

For all copying, reprint, or republication permission, write to: Copyrights and Permissions Department, Informatics Society, secretariat@infsoc.org.

Publisher

Address: Informatics Laboratory, 3-41 Tsujimachi, Kitaku, Nagoya 462-0032, Japan

E-mail: secretariat@infsoc.org

CONTENTS